Drainage divide migration and implications for climate and biodiversity

Chuanqi He[1,2,3†], Jean Braun[1], Hui Tang[1], Xiaoping Yuan[2],
Esteban Acevedo-Trejos[1], Richard F. Ott[1], Gaia Stucky de Quay[3]

[1]German Research Centre for Geosciences, Potsdam, Germany
[2]School of Earth Sciences, China University of Geosciences, Wuhan, China
[3]Department of Earth, Atmospheric & Planetary Sciences, Massachusetts Institute of Technology, Cambridge, MA USA

†email: chuanqihe@outlook.com

Abstract

Drainage divides separate Earth's surface into individual river basins. Divide migration impacts the evolution of landforms, regional climate, ecosystems, and biodiversity. In this Review, we assess the processes and dynamics of divide migration, and offer insights into the impact on climate and biodiversity. Drainage divides are not static, they can move through the processes of gradual migration that is continuous in unsteady landscapes, or sudden through infrequent river capture events. Divides tend to move in the direction of slower erosion, faster uplift, or with horizontal tectonic advection, with rates typically ranging between 0.001 to 10 mm yr^{-1}, and a global average of 0.6 mm yr^{-1}. Evidence of river capture, such as a sharp change in flow direction with an upstream waterfall, can constrain divide migration history. Topographic metrics, such as cross-divide steepness, can predict the migration of drainage divides towards directions with a lower topographic steepness. Divide migration influences the spatial distribution of regional precipitation, temperature, and topographic connectivity between species, thereby affecting biodiversity. For example, freshwater fish can migrate into a new drainage basin through river capture, potentially increasing the species richness. Future research should couple advanced landscape evolution models and observations from field and remote sensing to better investigate divide migration dynamics.

Website Summary:

Drainage divides—the topographic boundary separating surface water flow—are dynamic features of Earth's surface that shape hydrological processes, sediment transport, carbon cycles, and geographic connectivity of ecosystems. This Review explores the dynamics of divide migration and its implications.

Key points

1) Drainage divides can move through gradual migration and occasional river capture. Drainage divides tend to move in the direction of slower erosion, faster uplift, or with horizontal tectonic advection.

2) Tectonics and erosion jointly influence divide dynamics and mountain asymmetry. Mountain asymmetry can increase with tectonic convergence velocity, while climate can both increase and decrease mountain asymmetry.

4) Evidence of river capture can decode divide motion history. Cross-divide steepness metrics and χ-value maps (drainage-area normalised distance along a river channel) can predict short-term and long-term divide stability, respectively.

5) Main drainage divide position of mountains affects spatial patterns of rainfall via orographic effect and temperature through altitude-temperature relationship, thereby influencing the richness and type of species.

6) River capture events can promote species richness in the expanding basins, but can decrease biodiversity in the shrinking catchments. However, overall diversity tends to increase due to

vicariant speciation in the expanding catchment.

Introduction

Drainage divides are the topographic boundary separating surface water flow into discrete drainage basins. They form at all spatial scales, being a boundary across continents (Fig. 1a), or between catchments[G] (Fig. 1b), and streams (Fig. 1c). Time-series remote sensing imageries, topographic analyses, and erosion rate measurements demonstrate that divides are not static but highly mobile[1-3]. The horizontal motion of drainage divides can result in changing river networks with substantial implications for the hydrological processes[4], sediment transport[5], carbon cycle[6], and the geographic connectivity between ecosystems and species[7-10]. For example, the position and movement of drainage divides can influence species richness by altering geographic connectivity and the patterns of topographic relief, rainfall, and temperature[11-15]. Understanding how and why drainage divides evolve can help reveal the fundamental geological and hydrological processes shaping the Earth's surface.

Drainage divide migration is typically a gradual and continuous process proceeding at slow rates, typically less than one meter every 1000 years[3,16,17]. By contrast, river capture events are more sporadic and sudden, occurring when a river breaches its drainage divide and connects with another river[18]. Gradual divide motion, in combination with sporadic river capture events, determines the positions of divides and the planform layout of river systems. Physical[19,20] and numerical experiments[21-23] reveal that tectonic movements[24-26], climate[27], and lithology[28,29] can influence divide mobility. In tectonically inactive regions, divides shift toward the side with lower erosion rates[30]. For instance, in a symmetrical mountain range, contrasting precipitation on either side of the mountain will push the main drainage divide[G] towards the drier side[19]. This main drainage divide migration, in turn, can alter the spatial distribution of precipitation through the orographic effect, further adding to the complexity of drainage divide migration[27].

The migration of drainage divides was first recognised in the Rocky Mountains around the 1870s[30]. Since then, the advancement of remote sensing, geologic dating, and numerical simulations, have triggered a proliferation research into the dynamics of divide movement[21,31]. For example, a novel and effective method to predict the direction of divide movement in 2014[32] boosted divide migration to become a trending research topic in geomorphology[33]. Thereafter, the number of methods used to decode divide migration histories, predict their future mobility[32,34,35], and constrain the rates of divide horizontal migration[3,4,36] has rapidly increased. However, a synopsis is required to understand and consolidate these methods and the interactions among the competing factors that influence divide motion.

In this Review, we aim to provide an overview of the mechanisms and forcings of drainage divide migration and explore the implications on climate and biodiversity[G]. To better understand the dynamics of divide migration, we evaluate their steady-state position and migration rate. Additionally, we provide an overview of the methods used for decoding divide migration history and predicting their future mobility. We build on the growing evidence showing how divide migration influences regional biodiversity[13,15,37], and explore the mechanisms of how the position and movement of drainage divides impacts regional rainfall, temperature, and ecosystems. Finally, we advocate for a research agenda integrating divide migration with ecosystems, geohazards, and planetary sciences.

The processes of divide migration

While drainage divides can move under various environments, the processes involved can be broadly categorised into two types. Divides can move through gradual migration (Fig. 2a) or river capture (Fig. 2b,c). Below we elaborate on the defining characteristics of these processes for divide motion with documented examples.

Gradual divide migration

Materials on hillslopes[G] move downslope through landslides, debris flows, rock falls, and soil creep. Located at the top of hillslopes, divides can move gradually during hillslope erosion[38] (Fig. 2a) or cross-divide differential uplift[39]. For example, a drainage divide in Taiwan shifted due to landsliding and asymmetric hillslope diffusion (Fig. 2d). The fastest divide motions

through gradual migration process are typically found in regions that have experienced catastrophic geologic or climatic events[1]. For instance, hundreds of landslide-induced divide motions were identified in the Himalaya (Mw7.8 Gorkha earthquake), the Tibetan Plateau (Mw7.9 Wenchuan earthquake), and Taiwan (Typhoon Morakot), with each landslide causing an average area exchange of 5000 m^2, ref.[1].

River capture

During river capture events, drainage area is transferred from the shrinking to the expanding catchment[G][40-42]. Based on how the divide is breached, river capture can be classified into bottom-up and top-down types[43]. In bottom-up capture, channels in the expanding catchment erode the divide through lateral meandering or channel head backward extension (Fig. 2b). When the divide breaching is completed, two originally separate rivers merge, resulting in a river capture. In contrast, in top-down capture, the breaching of the divide is induced by overtop erosion from the water flowing downwards across the divide (Fig. 2c). Tectonic tilting could facilitate water spilling over the divide into the adjacent catchment[43]. Increased water level due to sedimentation, channel blocking, or flooding might also cause the water to overflow across the divide. Both types of river capture typically form a pronounced flow direction change (elbow of capture), a knickpoint[G], and a wind gap[G] at the point of river connection (Fig. 2b,c). Following river capture, the knickpoint and wind gap migrate upstream through erosion[44,45]. The upstream migration of the wind gap can form a river channel with flow direction opposite to that before capture[46] (Fig. 2b,c).

A prominent example of bottom-up river capture occurred 350,000 years ago in the north margin of the Tibetan Plateau[47], which formed a new divide crossing the old river channel (Fig. 2e). The incision depth since this capture event is about 350 m, indicating an incision rate of 1 mm yr^{-1} near the capture point. This rate is over three times higher than the catchment-averaged erosion rate of ~0.3 mm yr^{-1}, ref.[47]. The discrepancy is likely caused by accelerated incision near the capture point, which can be attributed to a base level[G] fall resulting from this capture event.

Bottom-up river capture also had a crucial role in shaping the present Yellow River basin, the cradle of Chinese civilization[48]. The onset of the Mid-Pleistocene Climate Transition led to a drop in sea level[49], which accelerated the headward erosion in the Sanmen Gorge[48]. This erosion cut through the divide 1.3 million years ago[48], evolving the modern Yellow River into the sixth longest river globally.

An ongoing example of top-down river capture is occurring in South America (Supplementary Fig. 1). A drainage divide between the Amazon and Orinoco Basins is being eroded by seasonal overtop-flooding, which might have been occurring for a century and is still incomplete[50]. Once the river capture is complete, the drainage divide will shift 200 km towards the Orinoco Basin, causing the Amazon to increase its drainage area by 40,000 km^2, ref.[50]. In addition to this example, lake overflow is a typical case of top-down river capture[51-53].

In brief, drainage divides shift their position through two primary processes: gradual migration and river capture. While gradual migration often leaves few geomorphic traces (unless caused by landslides), river capture resulting from channel backward extension or overtop flows causes pronounced changes in the landscape. Features such as elbows of capture, knickpoint, wind gap, and reversed river channel can be used to reconstruct the history of river capture and associated divide migration.

Divide migration dynamics

Drainage divides are affected by multiple internal and external forcings, as well as their complex interplay and feedbacks[2,25,32]. Despite the intricate nature of these dynamics, under steady forcings, divides tend to reach a topographic steady state where tectonics and erosion are in balance[54]. The rate of drainage divide migration affects the time needed to reach steady state. To provide an overview of the dynamics of drainage divides, we examine the drivers of their movement, steady-state position, the timescale for reaching equilibrium, and the migration rate.

Drivers of divide migration

Tectonic drivers.

As a topographic feature, a drainage divide can move laterally when the elevation near the divide exceeds that of the original divide[2]. Tectonic processes (vertical uplift and horizontal tectonic advection[G]) and surface erosion are the primary drivers of divide lateral movement (Fig. 3), as they determine the elevation of a landscape[24,55,56]. Vertical uplift can influence divide mobility by modifying the topography directly (Fig. 3a). When cross-divide unequal uplift is sustained, the elevation of the fast-uplifting region will exceed the height of the previous divide, moving the divide to the area with faster uplift[39,57,58]. Meanwhile, the motion of bedrock not only has a vertical component but can also have a horizontal component[59-64]. Such a tectonic advection could drive the horizontal movement of every point in the landscape towards the fixed plate boundary[24,62]. Analogue[65] and numerical[24,25] experiments, as well as natural case study[66], indicate that during the transient phase of topographic evolution, drainage divides tend to move in the direction of advection (Fig. 3b), no matter the spatial distribution and magnitude of the advection velocity[25]. After drainage divide stabilises relative to the fixed plate boundary, its migration rate relative to the underlying rock equals the advection velocity but in the opposite direction[24,67].

Erosional drivers.

It has been known since 1877 that drainage divides are sensitive to cross-divide erosion differences and will migrate towards the side with slower erosion[30]. Topographic slope[68], rock properties[28], and climate[69] can influence surface erosion. Thus, these factors are considered to be erosional drivers to divide migration. To better illustrate the role of each element in influencing divide migration, we assume these factors are mutually independent. First, the average slopes on both sides of the divide determine the geometric disequilibrium. Steeper topography provides more erosive power and limits deposition, causing intensive erosion that leads to the divide moving towards the flatter side[25,30] (Fig. 3c). Second, divides tend to move to the side with hard lithologies such as granite[70-72] (Fig. 3d). Third, a wetter climate means more discharge, promoting vigorous physical and chemical erosion and triggering more frequent catastrophic events such as landslides and debris flows[73]. Also, as a glacier moves downslope, it erodes bedrock through plucking and abrasion[69]. Collectively, a cross-divide climate difference can move the divide to the side with less rainfall[19,27,21] (Fig. 3e) or glacial mass[74] (Fig. 3f).

Combined effects from multiple drivers.

As illustrated in the previous sub-sections, drainage divides tend to move towards faster uplift, horizontal advection, flatter topography, stronger rock, less rainfall and glacial mass (Fig. 3). However, in natural landscapes, drainage divide mobility is jointly affected by multiple drivers[25]. For instance, in Fig. 3a, non-uniform uplift is the only driver when the divide is in the centre. In this example, the faster uplift on the right side pushes the divide to the right. As the divide moves, the slope on both sides diverges, which tends to shift the divide to the left side with smaller slope. However, the unequal uplift makes a larger contribution, which drives the divide to continue moving towards the right. As the divide moves to the right, the contribution from asymmetric erosion to divide mobility increases due to the increasing cross-divide slope difference[25]. When the contribution from asymmetric erosion matches the contribution from unequal uplift, the divide reaches a steady state.

The Southern Alps of New Zealand is a classic example demonstrating the competition between tectonics and erosion in driving divide motion. The northwest and southeast sides of this range receive precipitation rates of approximately 12 and 1 m yr^{-1}, respectively[21]. Such a substantial cross-divide erosion difference tends to shift the main divide to the side with less precipitation in the southeast (Fig. 3e). However, westward tectonic motion eventually pushed the main divide close to the northwest coastline[21]. In the Southern Alps, the erosion contrast is not efficient enough to reverse the highly asymmetric mountains created by westward tectonic motion[59].

In addition, the complex internal feedback among multiple drivers also affects the dynamics of drainage divides. For example, consider the unequal rainfall scenario in Fig. 3e. Unequal rainfall will push the divide to the left side with a drier climate. Meanwhile, a wetter environment on the right is expected to result in more vegetation cover. However, vegetation cover is not always positively correlated with catchment-scale erosion rates, depending on climate zone and vegetation type[75]. Thus, if vegetation inhibits erosion, vegetation cover differences tend to push the divide to the right side (Fig. 3e). In contrast, if vegetation accelerates erosion, both vegetation and rainfall differences shift the divide leftwards. As a result, the complex trade-offs and correlations between factors influencing divide migration must be considered when analysing the dynamics of natural divides, especially in geologically and climatically complex regions.

Stable divide position and timescale

Mountain asymmetry in steady state.

Since catchment boundaries and the main drainage divide of a mountain range share the same dynamics (Fig. 3), we focus on the position and timescale of the main divide. Mountain asymmetry is a crucial feature of mountain ranges determined by the position of the main drainage divide (Fig. 1a). Although a perfect topographic steady state is unlikely to be attained[24,54], a long-wavelength topographic form can be reached with constant mean elevation and mountain asymmetry[56,60,76]. A convergent orogen (Fig. 4a) is a useful example for summarising the concept of stable mountain asymmetry resulting from surface erosion, advection, and uplift simultaneously[24,25,77]. The mantle and lithospheric processes can cause uneven uplift and horizontal advection of the topography, pushing the main drainage divide towards the fixed plate on the right (Fig. 4a). Mountain asymmetry in steady state is positively related to horizontal advection velocity[25,64] and the difference in uplift rate between two sides of the mountain range[25,78,79]. Convergence velocity sets the advection velocity and the magnitude of unequal uplift, indicating that the mountain asymmetry is expected to increase with convergence velocity[25,59] (Fig. 4b). With a uniform climate, tectonics and differential erosion tend to push the divide towards the retro-wedge and pro-wedge sides, respectively (Fig. 4a). In this case, dry climate means the erosion has less power to balance the tectonic motion[25], eventually resulting in a more asymmetric mountain range (Fig. 4b).

In contrast, when precipitation is asymmetric across the main drainage divide, climate can either enhance or counteract the effect of tectonics in defining mountain symmetry[59] (Fig. 4c). Specifically, less rainfall on the faster uplift side (the retro-wedge side) will lead to a more asymmetric mountain range, such as in the Olympic Mountains of the USA[59]. However, more rain on the retro-wedge side can offset the forcing of tectonics, resulting in a less asymmetric mountain range (Fig. 4c), such as in the Southern Alps of New Zealand[25,21,59]. If the cross-divide rainfall difference is substantial enough, it can dominate over tectonics, and the main divide will stabilise on the pro-wedge side of the mountain. In this case, stable mountain asymmetry increases with rainfall difference (Fig. 4c). The above discussion implicitly assumes that the uplift rate and climate are uniform along the strike of mountains. However, an along-strike variation in uplift or rainfall can further modify mountain asymmetry[23]. Due to these complex dynamics affecting drainage divides, asymmetric mountain ranges prevail in natural landscapes.

Timescale to reach steady state.

Tectonic and climatic forcings, rock types, geometric disequilibrium, and landscape size can influence the timescale a divide requires to achieve steady state, where divide movement ceases. The original topography is unlikely to control the stable mountain asymmetry but can influence the time to reach steady state[80]. The timescale of drainage divides to achieve steady state typically ranges between 100 thousand to 100 million years based on results from numerical models (5 ×10 km in size; Supplementary Fig. 2a), and decreases with increasing erodibility[22,59] (Supplementary Fig. 2b) and uplift rate[25,22,23]. A drainage divide in Tibet requires approximately 100 million years to attain stability, based on the measured divide migration rate (~1.2 mm yr^{-1}) and the distance (~120 km) between the current divide position and the inferred stable

location[16].

Furthermore, river profiles adjust to external perturbations typically faster than drainage divides (based on field observations[29,40] and numerical simulations[32,22]), meaning divides can still move even after the river profiles have reached quasi-equilibrium state. For example, the response time of river profiles in the Ozark dome, USA, are in the order of tens of million years, while drainage divides in the same region move on timescales of hundreds of million years[40].

The rates of divide migration

The rate of drainage divide horizontal motion has received less attention than the direction of divide motion, mainly due to the difficulty of obtaining accurate estimates in natural landscapes. However, since 2018, attempts have been made to determine divide migration rate using constraints from ^{10}Be concentrations[3,16,81,82], thermochronology[G][36], topographic analyses[83], analytical solutions[4,84,85], and numerical experiments[84,86].

For example, combining erosion rate and slope on both sides of a divide can be used to estimate divide migration rate[3,16]. The concentration of cosmogenic ^{10}Be measured from river sediments can provide a catchment-averaged erosion rate[87]. Applying this method, divide migration rates have been estimated in east Tibet (0.02–0.7 mm yr^{-1})[85], northeast Tibet (0–1.4 mm yr^{-1})[16], and the Andes (0.8–7.3 mm yr^{-1})[36] (Fig. 4d). One limitation of this approach is that the measurement of migration rate is sensitive to the scale used to measure the slope[3], obstructing the comparison between measurements using a different scale of slope.

Unlike divide migration rate estimated from ^{10}Be-derived erosion rates that typically integrate over the millennial timescale, thermochronology can average divide migration rate over millions of years[36,88]. For example, a drainage divide located in the glaciated Canadian Coast Mountains migrated 16 km in the past 1.5–4 million years[88], meaning the divide migration rate was 4–11 mm yr^{-1} (Fig. 4d). Additionally, a migration rate of 2–5 mm yr^{-1} over several million years was reported from Sierra de Aconquija (south Andes), consistent with the short-term migration rate of ~1–7 mm yr^{-1} estimated from the ^{10}Be-derived erosion rates[36] (Fig. 4d). The inversion of knickpoint migration in the Roan Plateau suggests a divide migration rate of 4 mm yr^{-1} over the past one million years[83]. Apart from natural observations, analytical solutions that rely on topographic and climatic parameters have been developed[4,84], yielding a similar range of divide migration rates with natural measurements[3,16,36] (Fig. 4d) and simulations[22,72]. Estimates of divide migration rates from various methods are mostly less than 10 mm yr^{-1}, suggesting that divide migration operates unassumingly on the Earth's surface. However, over geological timescales spanning millions of years, divide migration can introduce kilometer-scale perturbations to the plan-view layout of drainage systems. Furthermore, river capture has the potential to amplify disturbances caused by gradual divide migration on river networks.

Rift margin escarpments[G] are widely distributed on Earth (Supplementary Fig. 3a) and are ideal landscapes for measuring drainage divide migration rates. Due to the topographic contrast between the steep escarpment and the flat plateau (Supplementary Fig. 3b), the escarpments move inland. This topographic asymmetry can persist for over 100 million years[17,81,84]. For instance, the Blue Ridge Escarpment in eastern USA, formed approximately 200 million years ago, is still moving[3,89]. As escarpments retreat inland gradually, discrete river captures can accelerate the retreat process. Following river capture, the drainage divide jumps from the escarpment to the flat plateau[3,82]. Subsequently, divide migration ceases due to similar slope across the divide. Meanwhile, the escarpment retreats towards the divide due to a notable topographic contrast across the escarpment. Once the two features come into proximity, they initiate a next round of river capture. Therefore, although drainage divide migrates much faster than escarpment during captures[82], their long-term migration rates are similar. Erosion rates derived from ^{10}Be concentrations have been applied to estimate the rate of escarpment retreat to be 0.04−0.08 mm yr^{-1} for the Australian Escarpment[90] and up to 0.05 mm yr^{-1} along the Blue Ridge Escarpment[3], respectively (Fig. 4d). ^{10}Be concentrations have been interpreted as a horizontal mass flux that can quantify the migration rate of the divide-escarpment system,

yielding speeds of 0.2−1.9 mm yr^{-1} in India[81] and Madagascar[17] (Fig. 4d).

Divide migration rates tend to remain relatively stable during escarpment retreat[4,82,84]. For a non-escarpment landscape without advection, simulation results show that divide migration rate can decrease to zero as it approaches steady state (Supplementary Fig. 4). For the analysis of divide migration rates, it is essential to consider the reference frame. Under steady horizontal advection, the divide migration rate relative to the fixed plate boundary is expected to decrease towards zero. In contrast, the migration rate relative to the underlying rock can reach its maximum as the landscape achieves steady state[24,67]. Divide migration rates derived from erosion rates and topographic measurements are relative to the underlying rock (Fig. 4d). However, there are differences in the temporal and spatial response scales for different methods[3]. Additionally, the way of interpreting ^{10}Be concentrations in escarpment retreat analyses affects the estimates of divide migration rates[3,81]. Therefore, these points should be considered when comparing divide migration rates across different regions.

To summarise, the direction, stable position, response time, and rate of drainage divide migration are controlled by tectonics and erosion. Owing to the Earth's diverse tectonic regimes, climate, rock types, and topography, measured divide migration rates span four orders of magnitude (0.001-10 mm yr^{-1}). However, divide migration rates under various climatic and geological conditions remain to be investigated.

Assessing divide migration direction

Building on the discussion of divide migration processes and dynamics, we use this section to discuss the main strategies to assess divide migration history and estimate their future mobility.

Reconstructing divide motion history

River capture changes the topology of drainage networks, leaving observable signals such as elbow of capture[35,78], knickpoint[91,92], wind gap[47,93] (Fig. 5a), reversed river channel[46], sediment provenance of river deposits[94], and the genetic imprinting of freshwater species[95-98]. Evidence of river capture can be used to decode divide migration history regardless of tectonic and climatic conditions (Fig. 5a). For a river capture to occur, the headwater elevation of the expanding catchment must be lower than the shrinking catchment[G], which triggers a knickpoint at the capture point. This knickpoint will move upstream due to erosion. Therefore, a knickpoint at or upstream of a river elbow is typical evidence of river capture[42,78] (Fig. 5a). The distance between the knickpoint and the elbow of capture is positively correlated with the capture age, providing further insight into the history of the capture event. River capture commonly leaves a wind gap as the new divide where fluvial sediments of the pre-capture river can be preserved[93]. The upstream migration of the wind gap results in the reversal of the river channel between the wind gap and the elbow of capture[46] (Fig. 2b,c). River captures lead to the redistribution of sediments. Therefore, the provenance of sedimentary deposits can serve as evidence of capture[99]. River capture can lead to splits in lineages of riverine organisms, thus, their phylogenies can document the history of capture-related divide motion[98,100].

An example of combining various methods to reconstruct the history of river capture in East China is shown in Fig. 5b. Geologic dating of sediments suggests that the capture happened 80,000 years ago[35]. First, a 135° flow direction change in River 1 marks a noteworthy elbow of capture. Second, two knickpoints can be observed in rivers 1 and 2 upstream of the capture elbow. Third, the current divide between Rivers 2 and 3 is low and flat, a typical wind gap[35]. The wind gap formed at the elbow of capture and migrated upstream to its current location since the capture event[44]. Fourth, the dip directions of the imbricated cobbles in the pre-capture river terrace suggest that River 2 was flowing contrary to its current flow direction[35] (Fig. 2b). The example above illustrates how to use the evidence of river capture to decode a single divide motion event. Furthermore, with the evidence of a series of river captures, the location of a paleo-divide spanning hundreds of kilometres can be reconstructed, as illustrated in the Iberian Peninsula[92].

In addition to the evidence of river capture, a combination of time-series optical remote

sensing[101,102] and elevation data can reveal divide motion histories spanning days to decades[103] (Fig. 2d). This remote sensing method has helped identify 365 landslide-triggered divide migration events in Tibetan Plateau, Himalaya, and Taiwan[1]. Additionally, thermochronometry can be used to reconstruct the history of divide motion[88,104,105].

Predicting divide migration direction

Long-term prediction by χ-maps.

χ is a drainage-area normalised distance along a river channel[106] (Fig. 5c). A disparity in χ across a drainage divide predicts a difference in equilibrium elevation and erosion potential. Accordingly, divides are predicted to migrate to the side with a higher χ channel head, under uniform uplift, climate, and lithology conditions[32]. The χ value at the channel head is an integral over the entire catchment, thus reflecting divide mobility over a long timescale (millions of years)[32,34].

χ-maps are appealing because they allow a quick visual assessment of divide stability. χ-maps have been widely used in Europe[107-109], Americas[40,110,111], Asia[47,112,113], and Africa[17,114]. However, caution must be applied when interpreting χ-maps[32,34,115], because mountain ranges rarely exhibit uniform uplift, climate, and erodibility conditions. When the mean uplift rates, precipitation rates, and rock erodibilities along the entire flow path on both sides of the divide are similar, χ-map might still predict long-term divide stability. Additionally, for mountains with known uplift fields and rainfall patterns, modified χ-maps can predict divide stability under heterogeneous geologic and climatic environments[32,20,115,116]. Furthermore, a proper selection of base level[34,117] is required to avoid misinterpretation of χ-maps.

An example of χ-map used to predict the direction of a Colorado divide characterised by uniform climate and bedrock properties is shown in Fig. 5d[83]. The uplift rate can be assumed to be uniform within this small area without active faults. Strong contrast in channel head χ values suggests that the divide is moving towards the Roan Plateau[83].

Short-term prediction by cross-divide steepness metrics.

Cross-divide steepness metrics (relief, slope, elevation) measured only near drainage divides can predict divide mobility over a shorter timescale compared to χ-maps[30,34,118] that integrate geometry information to predict equilibrium elevation across entire basins. However, cross-divide steepness metrics do operate under the same principle as χ-maps, that the divide is sensitive to the cross-divide differences in erosional potential (Fig. 3c). Divides are predicted to move to the side with a lower topographic steepness until the difference across the divide becomes negligible[30,22] (Fig. 5e). Cross-divide steepness metrics are widely used to predict divide motion direction[66,117,119]. For example, in the Big Bear Plateau of California (Fig. 5f), the prediction of divide direction from cross-divide relief is consistent with χ-map and cross-divide erosion rate[34]. All metrics predict that the main drainage divide is moving towards the Big Bear Plateau, indicating the plateau is being consumed until the eventual disappearance of the plateau at steady state. TopoToolbox[120] provides a quick calculation of χ-maps and cross-divide steepness metrics.

In summary, river capture legacies, time-series remote sensing, and thermochronometry can help constrain the previous locations of drainage divides. χ-maps and cross-divide steepness metrics can predict the direction of divide migration. χ-maps are particularly suitable for predicting the migration direction over millions of years. For shorter prediction time scales (for example, several hundred thousand years), cross-divide steepness metrics might be more robust.

Implications for climate and biodiversity

As one of the highest features in a landscape, drainage divides can function as a barrier to atmospheric moisture transport[121] and biological dispersal[12,122]. For example, aquatic organisms are unlikely to traverse drainage divides. Consequently, drainage divides have a potential influence on regional climate and species distribution patterns over mountain and catchment

scales. Below we discuss the current knowledge of divide position and mobility impacts on regional climate and biodiversity.

Divide position affects climate

The main drainage divides can affect regional climate of mountains by altering atmospheric circulation[123,124]. When warm, moist air encounters mountains, it is forced to ascend (Fig. 6a). As the moist air rises[121,125], it cools and condenses, resulting in cloud formation and rainfall. Typically, much of the moisture is lost on the windward side of a mountain range, leading to a rainshadow effect on the leeward side. This process is known as orographic precipitation[126,127]. Hence, the main drainage divide that separates the windward and leeward sides is a substantial factor influencing the spatial distribution of rainfall[27]. Air temperature tends to reduce by approximately 6.5°C for every 1000 m increase in elevation, although other factors such as moisture content can influence the spatial temperature variability[124,128]. Main drainage divide establishes a temperature gradient between lowland and mountain top. Therefore, as one of the highest terrains in a mountain range, the main drainage divide generally serves as the minimum boundary for regional temperature (Fig. 6a).

We present two examples from the Himalaya and Madagascar to illustrate how the position of the main drainage divide can influence the spatial distribution of rainfall, temperature, and species richness. We chose these two regions not only for their relatively low human impacts, but also for the presence of a main drainage divide stretching several hundred kilometers separating the topography into two parts. The Indian monsoon is one of the most notable monsoon systems on Earth[129]. Warm and moist air from the Indian Ocean blows towards the Himalaya, creating orographic precipitation. Annual rainfall increases from 1 m yr^{-1} in the Indian plain to 4 m yr^{-1} at 4000 m elevation. However, it decreases to 2 m yr^{-1} at the main divide before stabilising at less than 0.5 m yr^{-1} on the Tibetan Plateau (Fig. 6b). Similar orographic rainfall occurs in Madagascar where the warm moisture from the Indian Ocean is forced up by the eastern margin of the island[130,131], resulting in more rainfall on the east side of the main divide (Fig. 6c). While the main divides in Himalaya and Madagascar do not receive the highest amount of regional precipitation, their position determines the overall relief on both sides of the mountain, affecting the location of rainfall patterns. Moreover, the main divides in both Himalaya and Madagascar have the lowest near-surface air temperature, making them temperature boundaries (Supplementary Fig. 5). In summary, although the mean elevation of the main divides in Himalaya (6000 m) and Madagascar (1500 m) differ substantially, both main divides have the lowest regional temperature and exert influence over precipitation patterns.

Drainage divides influence biodiversity

Mountain-scale species richness.

The broad elevation and climate gradients provided by mountains allow them to support 87% of mammal, bird, and amphibian species on just 25% of Earth's land surface[11,12]. The heterogeneity of habitats observed in high-relief regions fosters both the facilitation (cradles) and maintenance (museums) of high biodiversity[9,132,133]. As a potential biological and climatic barrier, the main drainage divide could influence the evolution and distribution of mountain species through its combined effects. First, the main divide can act as a barrier that impedes species dispersal, which could increase the risk of extinction as shown for freshwater organisms[134]. Second, the position of the main divide allocates habitat size, water availability, and nutrients essential to sustain species richness on both sides of the range. Third, mountain asymmetry determines the topographic relief that is positively related to species richness[9,133]. Last, the main divide can influence the diversity and composition of species on either side of the mountains by adjusting regional climate. The rainshadow side typically supports more drought-tolerant species, while the wet side tends to have more moisture-adapted species[9] (Fig. 6a). Similarly, since the main divide is generally associated with lower temperatures, it can be expected that species closer to the main divide are more cold-tolerant. However, the small-scale

diversity patterns across the divide and the general mechanisms driving them are less understood.

Himalaya[135,136] and Madagascar[137] are known for their complex multistaged uplift and climate change histories and extraordinary biodiversity[138,139]. The current divide positions in relation to the local climate and the spatial distribution of vertebrate diversity seem to coincide (Fig. 6b,c; Supplementary Fig. 5). Albeit this evidence invites us to draw relationships between them, a closer look at the spatial patterns show that differences emerge between and within the two regions. In the Himalaya, the maximum species richness and rainfall are achieved at 125 and 35 km south of the main divide, respectively (Fig. 6b). In contrast, in Madagascar, both maximum species richness and rainfall are achieved at the escarpment's edge, 16 km east of the main divide (Fig. 6c).

Global patterns of species richness in mountains exhibit a hump-shaped or decreasing trend with increasing elevation[140,141], implying that the main drainage divides are generally not the maximum boundary of species richness. In addition, various mechanisms have been evoked to explain the geographical patterns of species diversity[142] and elevational richness[143]. These mechanisms include climate or energy-related factors[144,145], environmental heterogeneity[146], diversification time and area[147], among others[142,148]. However, there is no clear consensus on which mechanism is most relevant[149]. Moreover, confounding effects related to covariation of physical variables with altitude[150], as well as the scale[151] and sampling[152,153] of species richness data can hinder our understanding of such patterns. Nevertheless, we consider it valuable that future research efforts are dedicated to gaining new insights into the mechanisms that link topography, climate, and biodiversity across divides. Building on this foundation, further predictions could be made regarding the potential impacts of main drainage divide migration on regional climate and biodiversity. Such efforts will be essential for informing effective conservation strategies in regions of high ecological importance.

Catchment-scale biodiversity.

Freshwater ecosystems offer the highest vertebrate species density on the planet, harbouring over 20% of vertebrate species within less than 1% of Earth's land surface[14,154]. Drainage divides can limit gene flow and promote endemism in freshwater and riverine species, particularly in fish[14,37,155]. Global datasets[14,154] and numerical models[134] support the notion that river captures can accelerate the diversification of fish[15,156]. Simulations suggest that a single river capture can have three effects on the richness of freshwater fish[97] (Fig. 6d). First, species richness in the expanding catchment can increase as the capture disrupts the drainage divide and enables species from the shrinking catchment to disperse and colonise the expanding basin. Second, species richness in the expanding catchment is further enhanced through vicariance, where certain fish become isolated from their ancestral population due to the newly established drainage divide. The effects of river capture on the vicariance of freshwater fish have been documented in New Zealand[95,157,158], North America[96], Himalayas[98], and the Amazon River basin[14,154,159]. Third, the number of species inhabiting the shrinking basin that lose drainage area can decrease due to the local extinction caused by the reduced habitat capacity and potential loss of lineage diversity[97] (Fig. 6d).

In summary, river capture events can promote species richness in the expanding basins and decrease the biodiversity in the shrinking catchments. However, overall species diversity tends to increase after capture due to vicariant speciation in the expanding catchment, then declines to match the habitat capacity (Fig. 6d). Nonetheless, it remains unclear whether river capture is a universal driver of diversity in other (non-fish) groups of freshwater or riverine life. Additionally, the role of other eco-evolutionary processes, such as competition[160-162] and hybridization[163,164], on species richness after river captures requires further research.

Summary and future perspectives

As one of the most dynamic topographic features, drainage divides highlight the fundamental interconnectivity between the lithosphere, hydrosphere, biosphere, and atmosphere. Drainage divides are not static, they can move through gradual migration and river capture (Fig. 2). Divides tend to move to the side with slower erosion (flatter topography, stronger rock, or dryer

climate), faster uplift, or along the direction of horizontal advection. The rate of drainage divide migration measured on Earth ranges between 0.001 to 10 mm yr^{-1}, with an average of 0.6 mm yr^{-1} (Fig. 4d). Evidence of river capture documents divide migration history (Fig. 5a,b), while topographic metrics can predict future divide mobility (Fig. 5c-f). The position of the main divide can shape spatial patterns of regional climate, which could also have implications for the diversity and type of life in mountainous areas (Fig. 6). Additionally, the reorganisation of drainage divides can promote the richness of freshwater species by their combined effects on dispersal, speciation, and extinction.

Previous physical and numerical simulations of divide migration were typically performed by directly setting tectonic and rainfall conditions, under which topography evolves through river incision and hillslope erosion processes. To better capture the complex dynamics controlling divide mobility, future research could establish coupled numerical models of geodynamics[55,56,165], surface processes with sediment deposition[166], and orographic precipitation[27,167]. Such coupled models can more accurately predict the future direction, rates, and stable position of divide movements in natural mountain ranges. For example, running the coupled models over sufficiently long periods can provide crucial estimates of the time needed for a divide to reach topographic steady state, and predict the stable position of the main drainage divide, which defines mountain asymmetry. Furthermore, the proposed coupled models with inverse analysis techniques[168] can help to reconstruct the migration history of drainage divides in natural mountain ranges.

Further efforts are required to enhance comprehension of the influence of divide migration on regional climate and species richness. For example, biological evolutionary processes[97] and orographic effects[27] could be incorporated into landscape evolution models[167] to better examine how the types and diversity of mountain biota evolve with divide migration and the associated changes in precipitation. This integration can shed light on the mechanisms underlying the impacts of divide movement on species dispersal, speciation, and extinction. Additionally, during escarpment retreat, river capture can forge a waterway for isolated aquatic organisms from the plateau to travel to the steep escarpment with abruptly contrasting climate and topography. The impacts of river capture across escarpments on biodiversity, and links between the timescale of biological divergence and escarpment retreat rates, warrant further investigation. Such investigations would necessitate integrating simulations of escarpment retreat[4,82,84], modelling the impacts of capture on aquatic biota[97], measuring divide migration rates[3,81], and sequencing the genomes of aquatic organisms[169].

Under changing climate, frequent extreme events such as floods and landslides can lead to catastrophic top-down and bottom-up river captures[50] (Fig. 2b,c). Therefore, gaining deeper insights into the societal effects of divide motion related to river capture is essential to ensure public safety. Glacial lakes have grown rapidly due to anthropogenic global warming, exposing 15 million people to the threat of glacial lake-outburst floods[170-173], a risk typically associated with top-down river capture (Fig. 2c). Meanwhile, river capture can not only cause a permanent water shortage in the shrinking catchment (Fig. 2b,c), but also lower the water table in the expanding catchment. The latter effect has led to the abandonment of ancient Chinese cities[174]. Future efforts could move toward developing numerical models to simulate both top-down and bottom-up river capture processes. This complex challenge requires data integration across disciplines to represent critical factors like climate, hydrology, geology, and topography. With continued model refinement and validation against empirical observations, researchers might be able to establish digital twin[G] framework[175,176] for understanding and managing river capture risks in populated regions, especially in low-relief catchments with high river capture potential[43,50,134].

Beyond Earth, Mars exhibits abundant evidence of fluvial activity[177-180] that ceased around 3.7 billion years ago[181,182]. The discrepancy between the current topographic divide and the inferred original impact crater rim[G] can record the gradual divide migration history (Supplementary Fig. 6). Martian surface preserves over 220 breached paleolakes[182,183], implying the prevalence of river captures in early wetter environments[184]. The average rate of divide migration was measured to be 0.01 mm yr^{-1} at 801 sites on the wall of ten young (less than 40 million years) Martian craters[185] (Supplementary Fig. 7). Future research could explore

the similarities and differences in divide dynamics on Earth and Mars. For example, an investigation could be conducted to compare the mechanism and rates of Martian crater rim retreat with escarpment retreat on Earth. Moreover, advances in constraining the tectonic uplift and advection of mountain ranges based on the position and mobility of its main drainage divide[25], could be adapted and applied to qualitatively constrain the climate of planetary bodies with pervasive erosional systems, such as Titan and ancient Mars (Supplementary Fig. 8).

Drainage divide migration is an inconspicuous process despite its prevalence and importance in shaping river networks and ecosystems. We advocate for future long-term studies related to drainage basins to raise the awareness about the impacts of divide migration. For instance, the composition and evolution of species in association with changes in drainage basins are still inconclusive. Therefore, it appears crucial to further extend these lines of research to better understand the impacts of divide migration on catchment ecosystems. Moreover, investigating the dynamics and processes of river capture events and communicating their effects to the public and policymakers remains of utmost importance, as these events can lead to the redistribution of water, potentially triggering floods in the expanding catchment and water resource scarcity in a shrinking basin.

References

1. Dahlquist, M. P., West, A. J. & Li, G. Landslide-driven drainage divide migration. *Geology* **46**, 403-406 (2018).
2. Scheingross, J. S., Limaye, A. B., McCoy, S. W. & Whittaker, A. C. The shaping of erosional landscapes by internal dynamics. *Nat. Rev. Earth Environ.* **1**, 661-676 (2020).
3. Stokes, M. F. et al. The erosional signature of drainage divide motion along the Blue Ridge escarpment. *J. Geophys. Res.: Earth Surf.* **128**, e2022JF006757 (2023).
4. Willett, S. D., McCoy, S. W. & Beeson, H. W. Transience of the north American high plains landscape and its impact on surface water. *Nature* **561**, 528-532 (2018).
5. Salles, T. et al. Hundred million years of landscape dynamics from catchment to global scale. *Science* **379**, 918-923 (2023).
6. Battin, T. J. et al. River ecosystem metabolism and carbon biogeochemistry in a changing world. *Nature* **613**, 449-459 (2023).
7. Craw, D., Upton, P., Burridge, C. P., Wallis, G. P. & Waters, J. M. Rapid biological speciation driven by tectonic evolution in New Zealand. *Nat. Geosci.* **9**, 140-144 (2015).
8. Deiner, K., Fronhofer, E. A., Machler, E., Walser, J. C. & Altermatt, F. Environmental DNA reveals that rivers are conveyer belts of biodiversity information. *Nat. Commun.* **7**, 12544 (2016).
9. Antonelli, A. et al. Geological and climatic influences on mountain biodiversity. *Nat. Geosci.* **11**, 718-725 (2018).
10. Musher, L. J. et al. River network rearrangements promote speciation in lowland Amazonian birds. *Sci. Adv.* **8**, eabn1099 (2022).
11. Fjeldså, J., Bowie, R. C. K. & Rahbek, C. The role of mountain ranges in the diversification of birds. *Annu. Rev. Ecol. Evol. Syst.* **43**, 249-265 (2012).
12. Rahbek, C. et al. Building mountain biodiversity: Geological and evolutionary processes. *Science* **365**, 1114-1119 (2019).
13. Salles, T. et al. Quaternary landscape dynamics boosted species dispersal across Southeast Asia. *Commun. Earth Environ.* **2**, 240 (2021).
14. Val, P., Lyons, N. J., Gasparini, N., Willenbring, J. K. & Albert, J. S. Landscape evolution as a diversification driver in freshwater fishes. *Front. Ecol. Evol.* **9**, 788328 (2022).

15. Cassemiro, F. A. S. et al. Landscape dynamics and diversification of the megadiverse South American freshwater fish fauna. *PNAS* **120**, e2211974120 (2023).
16. Hu, K. et al. Covariation of cross-divide differences in denudation rate and χ: Implications for drainage basin reorganization in the Qilian Shan, northeast Tibet. *Earth Planet. Sci. Lett.* **562**, 116812 (2021).
17. Wang, Y., Willett, S. D., Wu, D., Haghipour, N. & Christl, M. Retreat of the great escarpment of Madagascar from geomorphic analysis and cosmogenic ^{10}Be concentrations. *Geochem. Geophys. Geosyst.* **22**, e2021GC009979 (2021).
18. Davis, D. M. A river-pirate. *Science* **13**, 108-109 (1889).
19. Bonnet, S. Shrinking and splitting of drainage basins in orogenic landscapes from the migration of the main drainage divide. *Nat. Geosci.* **2**, 766-771 (2009).
20. Habousha, K., Goren, L., Nativ, R. & Gruber, C. Plan-form evolution of drainage basins in response to tectonic changes: Insights from experimental and numerical landscapes. *J. Geophys. Res.: Earth Surf.* **128**, e2022JF006876 (2023).
21. Goren, L., Willett, S. D., Herman, F. & Braun, J. Coupled numerical-analytical approach to landscape evolution modeling. *Earth Surf. Process. Landf.* **39**, 522-545 (2014).
22. Whipple, K. X., Forte, A. M., DiBiase, R. A., Gasparini, N. M. & Ouimet, W. B. Timescales of landscape response to divide migration and drainage capture: Implications for the role of divide mobility in landscape evolution. *J. Geophys. Res.: Earth Surf.* **122**, 248-273 (2017).
23. He, C. et al. Landscape response to normal fault linkage: Insights from numerical modeling. *Geomorphology* **388**, 107796 (2021).
24. Willett, S. D., Slingerland, R. & Hovius, N. Uplift, shortening, and steady state topography in active mountain belts. *Am. J. Sci.* **301**, 455-485 (2001).
25. He, C. et al. Constraining tectonic uplift and advection from the main drainage divide of a mountain belt. *Nat. Commun.* **12**, 544 (2021).
26. Lanari, R., Reitano, R., Faccenna, C., Agostinetti, N. P. & Ballato, P. Surface and crustal response to deep subduction dynamics: Insights from the Apennines, Italy. *Tectonics* **42**, e2022TC007461 (2023).
27. Hergarten, S. & Robl, J. The linear feedback precipitation model (LFPM 1.0) – a simple and efficient model for orographic precipitation in the context of landform evolution modeling. *Geosci. Model Dev.* **15**, 2063-2084 (2022).
28. Bernard, T., Sinclair, H. D., Gailleton, B., Mudd, S. M. & Ford, M. Lithological control on the post-orogenic topography and erosion history of the Pyrenees. *Earth Planet. Sci. Lett.* **518**, 53-66 (2019).
29. Seagren, E. G. & Schoenbohm, L. M. Base level and lithologic control of drainage reorganization in the Sierra de las Planchadas, NW Argentina. *J. Geophys. Res.: Earth Surf.* **124**, 1516-1539 (2019).
30. Gilbert, G. K. *Report on the geology of the Henry Mountains* (Government Printing Office, 1877).
31. Val, P. et al. Erosion of an active fault scarp leads to drainage capture in the Amazon region, Brazil. *Earth Surf. Process. Landf.* **39**, 1062-1074 (2014).
32. Willett, S. D., McCoy, S. W., Perron, J. T., Goren, L. & Chen, C. Y. Dynamic reorganization of river basins. *Science* **343**, 1248765 (2014).
33. Liu, Z. et al. Quantitative analysis of tectonic geomorphology research based on Web of Science from 1981 to 2021. *Remote Sens.* **14**, 5227 (2022).

34. Forte, A. M. & Whipple, K. X. Criteria and tools for determining drainage divide stability. *Earth Planet. Sci. Lett.* **493**, 102-117 (2018).
35. Fan, N. et al. Abrupt drainage basin reorganization following a Pleistocene river capture. *Nat. Commun.* **9**, 3756 (2018).
36. Schildgen, T. F. et al. Quantifying drainage-divide migration from orographic rainfall over geologic timescales: Sierra de Aconquija, southern Central Andes. *Earth Planet. Sci. Lett.* **579**, 117345 (2022).
37. Rico, C. N., Hoagstrom, C. W., Elías, D. J., McMahan, C. D. & Matamoros, W. A. Biotic regionalization of freshwater fishes in Northern Middle America highlights high beta diversity created by prominent biogeographic barriers. *Front. Biogeogr.* **14**, e58095 (2022).
38. de Lavaissière, L., Bonnet, S., Guyez, A. & Davy, P. Autogenic knickpoints in laboratory landscape experiments. *Earth Surf. Dyn.* **10**, 229-246 (2022).
39. O'Hara, D., Karlstrom, L. & Roering, J. J. Distributed landscape response to localized uplift and the fragility of steady states. *Earth Planet. Sci. Lett.* **506**, 243-254 (2019).
40. Beeson, H. W., McCoy, S. W. & Keen-Zebert, A. Geometric disequilibrium of river basins produces long-lived transient landscapes. *Earth Planet. Sci. Lett.* **475**, 34-43 (2017).
41. Pérez-Consuegra, N. et al. Neogene variations in slab geometry drive topographic change and drainage reorganization in the Northern Andes of Colombia. *Global Planet. Change* **206**, 103641 (2021).
42. Seagren, E. G. & Schoenbohm, L. M. Drainage reorganization across the Puna Plateau margin (NW Argentina): Implications for the preservation of orogenic plateaus. *J. Geophys. Res.: Earth Surf.* **126**, e2021JF006147 (2021).
43. Bishop, P. Drainage rearrangement by river capture, beheading and diversion. *Prog. Phys. Geogr.* **19**, 449-473 (1995).
44. Shelef, E. & Goren, L. The rate and extent of wind-gap migration regulated by tributary confluences and avulsions. *Earth Surf. Dyn.* **9**, 687-700 (2021).
45. Harel, E., Goren, L., Crouvi, O., Ginat, H. & Shelef, E. Drainage reorganization induces deviations in the scaling between valley width and drainage area. *Earth Surf. Dyn.* **10**, 875-894 (2022).
46. Harel, E., Goren, L., Shelef, E. & Ginat, H. Drainage reversal toward cliffs induced by lateral lithologic differences. *Geology* **47**, 928-932 (2019).
47. Su, Q., Wang, X., Lu, H., Zhang, H. & Xie, H. River piracy and its geomorphic effects in the northern Qilian Shan, northeastern Qinghai-Tibet Plateau. *Palaeogeogr. Palaeoclimatol. Palaeoecol.* **601**, 111147 (2022).
48. Wang, X. et al. Did the modern Yellow River form at the Mid-Pleistocene transition? *Sci. Bull.* **67**, 1603-1610 (2022).
49. Miller, K. G. et al. The Phanerozoic record of global sea-level change. *Science* **310**, 1293-1298 (2005).
50. Stokes, M. F., Goldberg, S. L. & Perron, J. T. Ongoing river capture in the Amazon. *Geophys. Res. Lett.* **45**, 5545-5552 (2018).
51. Craddock, W. H. et al. Rapid fluvial incision along the Yellow River during headward basin integration. *Nat. Geosci.* **3**, 209-213 (2010).
52. Geurts, A. H. et al. Drainage integration and sediment dispersal in active continental rifts: A numerical modelling study of the central Italian Apennines. *Basin Res.* **30**, 965-989 (2018).
53. Hilgendorf, Z., Wells, G., Larson, P. H., Millett, J. & Kohout, M. From basins to rivers:

Understanding the revitalization and significance of top-down drainage integration mechanisms in drainage basin evolution. *Geomorphology* **352**, 107020 (2020).

54. Tejedor, A., Singh, A., Zaliapin, I., Densmore, A. L. & Foufoula-Georgiou, E. Scale-dependent erosional patterns in steady-state and transient-state landscapes. *Sci. Adv.* **3**, e1701683 (2017).
55. Bahadori, A. et al. Coupled influence of tectonics, climate, and surface processes on landscape evolution in southwestern North America. *Nat. Commun.* **13**, 4437 (2022).
56. Wolf, S. G., Huismans, R. S., Braun, J. & Yuan, X. Topography of mountain belts controlled by rheology and surface processes. *Nature* **606**, 516-521 (2022).
57. Su, Q., Wang, X., Lu, H. & Xie, H. Dynamic divide migration as a response to asymmetric uplift: An example from the Zhongtiao Shan, north China. *Remote Sens.* **12**, 4188 (2020).
58. Zhou, C., Tan, X., Liu, Y. & Shi, F. A cross-divide contrast index (C) for assessing controls on the main drainage divide stability of a mountain belt. *Geomorphology* **398**, 108071 (2022).
59. Willett, S. D. Orogeny and orography: The effects of erosion on the structure of mountain belts. *J. Geophys. Res.: Solid Earth* **104**, 28957-28981 (1999).
60. Willett, S. D. & Brandon, M. T. On steady states in mountain belts. *Geology* **30**, 175-178 (2002).
61. Castelltort, S. et al. River drainage patterns in the New Zealand Alps primarily controlled by plate tectonic strain. *Nat. Geosci.* **5**, 744-748 (2012).
62. Eizenhöfer, P. R., McQuarrie, N., Shelef, E. & Ehlers, T. A. Landscape response to lateral advection in convergent orogens over geologic time scales. *J. Geophys. Res.: Earth Surf.* **124**, 2056-2078 (2019).
63. Brune, S. et al. Geodynamics of continental rift initiation and evolution. *Nat. Rev. Earth Environ.* **4**, 235-253 (2023).
64. Mitchell, N. & Forte, A. M. Tectonic advection of contacts enhances landscape transience. *Earth Surf. Process. Landf.* **48**, 1450-1469 (2023).
65. Reitano, R. et al. Sediment recycling and the evolution of analog orogenic wedges. *Tectonics* **41**, e2021TC006951 (2022).
66. Chen, Y. et al. Evolution of eastern Tibetan river systems is driven by the indentation of India. *Commun. Earth Environ.* **2**, 256 (2021).
67. Hoskins, A. M., Attal, M., Mudd, S. M. & Castillo, M. Topographic response to horizontal advection in normal fault-bound mountain ranges. *J. Geophys. Res.: Earth Surf.* **128**, e2023JF007126 (2023).
68. Leonard, J. S., Whipple, K. X. & Heimsath, A. M. Isolating climatic, tectonic, and lithologic controls on mountain landscape evolution. *Sci. Adv.* **9**, eadd8915 (2023).
69. Herman, F., De Doncker, F., Delaney, I., Prasicek, G. & Koppes, M. The impact of glaciers on mountain erosion. *Nat. Rev. Earth Environ.* **2**, 422-435 (2021).
70. Giachetta, E., Refice, A., Capolongo, D., Gasparini, N. M. & Pazzaglia, F. J. Orogen-scale drainage network evolution and response to erodibility changes: insights from numerical experiments. *Earth Surf. Processes Landforms* **39**, 1259-1268 (2014).
71. Zondervan, J. R., Stokes, M., Boulton, S. J., Telfer, M. W. & Mather, A. E. Rock strength and structural controls on fluvial erodibility: Implications for drainage divide mobility in a collisional mountain belt. *Earth Planet. Sci. Lett.* **538**, 116221 (2020).
72. Bernard, T., Sinclair, H. D., Gailleton, B. & Fox, M. Formation of longitudinal river valleys and the fixing of drainage divides in response to exhumation of crystalline basement. *Geophys. Res. Lett.* **48**, e2020GL092210 (2021).

73. Perron, J. T. Climate and the pace of erosional landscape evolution. *Annu. Rev. Earth Planet. Sci.* **45**, 561-591 (2017).
74. Lai, J. & Huppert, K. Asymmetric glaciation, divide migration, and postglacial fluvial response times in the Qilian Shan. *Geology* **51**, 860-864 (2023).
75. Starke, J., Ehlers, T. A. & Schaller, M. Latitudinal effect of vegetation on erosion rates identified along western South America. *Science* **367**, 1358-1361 (2020).
76. Perron, J. T., Richardson, P. W., Ferrier, K. L. & Lapotre, M. The root of branching river networks. *Nature* **492**, 100-103 (2012).
77. Braun, J., Herman, F. & Batt, G. Kinematic strain localization. *Earth Planet. Sci. Lett.* **300**, 197-204 (2010).
78. He, C. et al. Divide migration in response to asymmetric uplift: Insights from the Wula Shan horst, North China. *Geomorphology* **339**, 44-57 (2019).
79. Shi, F., Tan, X., Zhou, C. & Liu, Y. Impact of asymmetric uplift on mountain asymmetry: Analytical solution, numerical modeling, and natural examples. *Geomorphology* **389**, 107862 (2021).
80. Perron, J. T. & Fagherazzi, S. The legacy of initial conditions in landscape evolution. *Earth Surf. Process. Landf.* **37**, 52-63 (2012).
81. Wang, Y. & Willett, S. D. Escarpment retreat rates derived from detrital cosmogenic nuclide concentrations. *Earth Surf. Dyn.* **9**, 1301-1322 (2021).
82. Wang, Y., Willett, S. D. & Wu, D. The role of weathering on morphology and rates of escarpment retreat of the rift margin of Madagascar. *J. Geophys. Res.: Earth Surf.* **128**, e2022JF007001 (2023).
83. Schwanghart, W. & Scherler, D. Divide mobility controls knickpoint migration on the Roan Plateau (Colorado, USA). *Geology* **48**, 698-702 (2020).
84. Braun, J. A review of numerical modeling studies of passive margin escarpments leading to a new analytical expression for the rate of escarpment migration velocity. *Gondwana Res.* **53**, 209-224 (2018).
85. Zhou, C. et al. Ongoing westward migration of drainage divides in eastern Tibet, quantified from topographic analysis. *Geomorphology* **402**, 108123 (2022).
86. Ye, Y., Tan, X. & Zhou, C. Initial topography matters in drainage divide migration analysis: Insights from numerical simulations and natural examples. *Geomorphology* **409**, 108266 (2022).
87. Balco, G., Stone, J. O., Lifton, N. A. & Dunai, T. J. A complete and easily accessible means of calculating surface exposure ages or erosion rates from ^{10}Be and ^{26}Al measurements. *Quat. Geochronol.* **3**, 174-195 (2008).
88. Ehlers, T. A., Farley, K. A., Rusmore, M. E. & Woodsworth, G. J. Apatite (U-Th)/He signal of large-magnitude accelerated glacial erosion, southwest British Columbia. *Geology* **34**, 765-768 (2006).
89. Linari, C. L. et al. Rates of erosion and landscape change along the Blue Ridge escarpment, southern Appalachian Mountains, estimated from in situ cosmogenic ^{10}Be. *Earth Surf. Process. Landforms* **42**, 928-940 (2017).
90. Godard, V., Dosseto, A., Fleury, J., Bellier, O. & Siame, L. Transient landscape dynamics across the Southeastern Australian Escarpment. *Earth Planet. Sci. Lett.* **506**, 397-406 (2019).
91. Struth, L., Teixell, A., Owen, L. A. & Babault, J. Plateau reduction by drainage divide migration in the Eastern Cordillera of Colombia defined by morphometry and ^{10}Be terrestrial cosmogenic

nuclides. *Earth Surf. Process. Landf.* **42**, 1155-1170 (2017).
92. Vacherat, A., Bonnet, S. & Mouthereau, F. Drainage reorganization and divide migration induced by the excavation of the Ebro basin (NE Spain). *Earth Surf. Dyn.* **6**, 369-387 (2018).
93. Struth, L., Giachetta, E., Willett, S. D., Owen, L. A. & Tesón, E. Quaternary drainage network reorganization in the Colombian Eastern Cordillera plateau. *Earth Surf. Process. Landf.* **45**, 1789-1804 (2020).
94. Prince, P. S., Spotila, J. A. & Henika, W. S. Stream capture as driver of transient landscape evolution in a tectonically quiescent setting. *Geology* **39**, 823-826 (2011).
95. Burridge, C. P., Craw, D. & Waters, J. M. River capture, range expansion, and cladogenesis: The genetic signature of freshwater vicariance. *Evolution* **60**, 1038-1049 (2007).
96. Bossu, C. M., Beaulieu, J. M., Ceas, P. A. & Near, T. J. Explicit tests of palaeodrainage connections of southeastern North America and the historical biogeography of Orangethroat Darters (Percidae: Etheostoma: Ceasia). *Mol. Ecol.* **22**, 5397-5417 (2013).
97. Stokes, M. F. & Perron, J. T. Modeling the evolution of aquatic organisms in dynamic river basins. *J. Geophys. Res.: Earth Surf.* **125**, e2020JF005652 (2020).
98. Li, X. et al. Genetic memory of fishes on river development in Himalayas. *Quat. Sci.* **43**, 819-837 (in Chinese with English abstract) (2023).
99. Fan, N. et al. Timing of river capture in major Yangtze River tributaries: Insights from sediment provenance and morphometric indices. *Geomorphology* **392**, 107915 (2021).
100. Lima, S. M. Q. et al. Headwater capture evidenced by paleo-rivers reconstruction and population genetic structure of the armored catfish (Pareiorhaphis garbei) in the Serra do Mar Mountains of southeastern Brazil. *Front. Genet.* **8**, 199 (2017).
101. Shugar, D. H. et al. River piracy and drainage basin reorganization led by climate-driven glacier retreat. *Nat. Geosci.* **10**, 370-375 (2017).
102. Chen, C. H., Shyu, J. B. H., Willett, S. D. & Chen, C. Y. Structural control on drainage pattern development of the western Taiwan orogenic wedge. *Earth Surf. Process. Landf.* **48**, 1830-1844 (2023).
103. Rodrigues Salgado, A. A., Ribeiro Marent, B. & Paixão, R. W. Large rivers, slow drainage rearrangements: The ongoing fluvial piracy of a major river by its tributary in the Branco river basin-northern Amazon. *J. South Am. Earth Sci.* **112**, 103598 (2021).
104. Simon-Labric, T. et al. Low-temperature thermochronologic signature of range-divide migration and breaching in the North Cascades. *Lithosphere* **6**, 473-482 (2014).
105. Mark, C., Cogné, N. & Chew, D. Tracking exhumation and drainage divide migration of the Western Alps: A test of the apatite U-Pb thermochronometer as a detrital provenance tool. *Geol. Soc. Am. Bull.* **128**, 1439-1460 (2016).
106. Perron, J. T. & Royden, L. An integral approach to bedrock river profile analysis. *Earth Surf. Process. Landf.* **38**, 570-576 (2013).
107. Winterberg, S. & Willett, S. D. Greater Alpine river network evolution, interpretations based on novel drainage analysis. *Swiss J. Geosci.* **112**, 3-22 (2019).
108. Diercks, M.-L., Stanek, K., Domínguez-Gonzalez, L. & Ehling, B. Quaternary landscape evolution and tectonics in Central Germany – A case study of the Harz. *Geomorphology* **388**, 107794 (2021).
109. Gailleton, B., Mudd, S. M., Clubb, F. J., Grieve, S. W. D. & Hurst, M. D. Impact of changing concavity indices on channel steepness and divide migration metrics. *J. Geophys. Res.: Earth*

Surf. **126**, e2020JF006060 (2021).
110. DeLong, S. B., Hilley, G. E., Prentice, C. S., Crosby, C. J. & Yokelson, I. N. Geomorphology, denudation rates, and stream channel profiles reveal patterns of mountain building adjacent to the San Andreas fault in northern California, USA. *Geol. Soc. Am. Bull.* **129**, 732-749 (2017).
111. García-Delgado, H. & Velandia, F. Tectonic geomorphology of the Serranía de San Lucas (central Cordillera): Regional implications for active tectonics and drainage rearrangement in the northern Andes. *Geomorphology* **349**, 106914 (2020).
112. He, C. et al. Geomorphological signatures of the evolution of active normal faults along the Langshan Mountains, North China. *Geodin. Acta* **30**, 163-182 (2018).
113. Wahyudi, D. R., Sinclair, H. D. & Mudd, S. M. Progressive evolution of thrust fold topography in the frontal Himalaya. *Geomorphology* **384**, 107717 (2021).
114. Amine, A., El Ouardi, H., Zebari, M. & El Makrini, H. Active tectonics in the Moulay Idriss Massif (south Rifian Ridges, NW Morocco): New insights from geomorphic indices and drainage pattern analysis. *J. Afr. Earth. Sci.* **167**, 103833 (2020).
115. Wu, Y., Yang, R., He, C. & He, J. Caution on determining divide migration from cross-divide contrast in χ. *Geol. J.* **57**, 4090-4098 (2022).
116. Zhou, C. & Tan, X. Quantifying the influence of asymmetric uplift, base level elevation, and erodibility on cross-divide χ difference. *Geomorphology* **427**, 108634 (2023).
117. Pai, M. O. D., Salgado, A. A. R., de Sordi, M. V., de Carvalho Junior, O. A. & de Paula, E. V. Comparing morphological investigation with χ index and Gilbert metrics for analysis of drainage rearrangement and divide migration in inland plateaus. *Geomorphology* **423**, 108554 (2023).
118. Scherler, D. & Schwanghart, W. Drainage divide networks – Part 1: Identification and ordering in digital elevation models. *Earth Surf. Dynam.* **8**, 245-259 (2020).
119. Alves, F. C., Stokes, M., Boulton, S. J., de Fátima Rossetti, D. & de Morisson Valeriano, M. Post-rift geomorphological evolution of a passive continental margin (Paraíba region, northeastern Brazil): Insights from river profile and drainage divide analysis. *Geomorphology* **414**, 108384 (2022).
120. Schwanghart, W. & Scherler, D. Short communication: TopoToolbox 2 – MATLAB-based software for topographic analysis and modeling in Earth surface sciences. *Earth Surf. Dyn.* **2**, 1-7 (2014).
121. Insel, N., Poulsen, C. J. & Ehlers, T. A. Influence of the Andes Mountains on south American moisture transport, convection, and precipitation. *Clim. Dyn.* **35**, 1477-1492 (2009).
122. Renny, M., Acosta, M. C. & Sérsic, A. N. Ancient climate changes and Andes uplift, rather than Last Glacial Maximum, affected distribution and genetic diversity patterns of the southernmost mycoheterotrophic plant Arachnitis uniflora Phil. (Corsiaceae). *Global Planet. Change* **208**, 103701 (2022).
123. Boos, W. R. & Pascale, S. Mechanical forcing of the North American monsoon by orography. *Nature* **599**, 611-615 (2021).
124. Pepin, N. C. et al. Climate changes and their elevational patterns in the mountains of the world. *Rev. Geophys.* **60**, e2020RG000730 (2022).
125. Mulch, A., Uba, C. E., Strecker, M. R., Schoenberg, R. & Chamberlain, C. P. Late Miocene climate variability and surface elevation in the central Andes. *Earth Planet. Sci. Lett.* **290**, 173-182 (2010).
126. Roe, G. H. Orographic precipitation. *Annu. Rev. Earth Planet. Sci.* **33**, 645-671 (2005).

127. Fisher, G. B. et al. Milankovitch-paced erosion in the southern Central Andes. *Nat. Commun.* **14**, 424 (2023).
128. Minder, J. R., Mote, P. W. & Lundquist, J. D. Surface temperature lapse rates over complex terrain: Lessons from the Cascade Mountains. *J. Geophys. Res.* **115**, D14122 (2010).
129. Hrudya, P. H., Varikoden, H. & Vishnu, R. A review on the Indian summer monsoon rainfall, variability and its association with ENSO and IOD. *Meteorol. Atmos. Phys.* **133**, 1-14 (2020).
130. Jury, M. R. Summer climate of Madagascar and monsoon pulsing of its vortex. *Meteorol. Atmos. Phys.* **128**, 117-129 (2015).
131. Arivelo, T. A. & Lin, Y.-L. Climatology of heavy orographic rainfall induced by tropical cyclones over Madagascar: From synoptic to mesoscale perspectives. *Earth Sci. Res.* **5**, 132-147 (2016).
132. Rangel, T. F. et al. Modeling the ecology and evolution of biodiversity: Biogeographical cradles, museums, and graves. *Science* **361**, 244 (2018).
133. Rahbek, C. et al. Humboldt's enigma: What causes global patterns of mountain biodiversity? *Science* **365**, 1108-1113 (2019).
134. Lyons, N. J., Val, P., Albert, J. S., Willenbring, J. K. & Gasparini, N. M. Topographic controls on divide migration, stream capture, and diversification in riverine life. *Earth Surf. Dyn.* **8**, 893-912 (2020).
135. Ding, L. et al. Timing and mechanisms of Tibetan Plateau uplift. *Nat. Rev. Earth Environ.* **3**, 652-667 (2022).
136. Wu, F. et al. Reorganization of Asian climate in relation to Tibetan Plateau uplift. *Nat. Rev. Earth Environ.* **3**, 684-700 (2022).
137. Ali, J. R. & Hedges, S. B. A review of geological evidence bearing on proposed Cenozoic land connections between Madagascar and Africa and its relevance to biogeography. *Earth Sci. Rev.* **232**, 104103 (2022).
138. Ding, W., Ree, R. H., Spicer, R. A. & Xing, Y. Ancient orogenic and monsoon-driven assembly of the world's richest temperate alpine flora. *Science* **369**, 578-581 (2020).
139. Antonelli, A. et al. Madagascar's extraordinary biodiversity: Evolution, distribution, and use. *Science* **378**, eabf0869 (2022).
140. Quintero, I. & Jetz, W. Global elevational diversity and diversification of birds. *Nature* **555**, 246-250 (2018).
141. Guo, Q. et al. Global variation in elevational diversity patterns. *Sci. Rep.* **3**, 3007 (2013).
142. Fine, P. V. A. Ecological and evolutionary drivers of geographic variation in species diversity. *Annu. Rev. Ecol. Evol. Syst.* **46**, 369-392 (2015).
143. Manish, K. et al. Elevational plant species richness patterns and their drivers across non-endemics, endemics and growth forms in the Eastern Himalaya. *J. Plant Res.* **130**, 829-844 (2017).
144. Hawkins, B. A. et al. Energy, water, and broad-scale geographic patterns of species richness. *Ecology* **84**, 3105-3117 (2003).
145. Field, R. et al. Spatial species-richness gradients across scales: a meta-analysis. *J. Biogeogr.* **36**, 132-147 (2009).
146. Stein, A., Gerstner, K. & Kreft, H. Environmental heterogeneity as a universal driver of species richness across taxa, biomes and spatial scales. *Ecol. Lett.* **17**, 866-880 (2014).
147. Mittelbach, G. G. et al. Evolution and the latitudinal diversity gradient: speciation, extinction and biogeography. *Ecol. Lett.* **10**, 315-331 (2007).

148. Körner, C. Mountain biodiversity, its causes and function. *AMBIO* **33**, 11-17 (2004).
149. Sanders, N. J. & Rahbek, C. The patterns and causes of elevational diversity gradients. *Ecography* **35**, 1-3 (2012).
150. Körner, C. The use of 'altitude' in ecological research. *Trends Ecol. Evol.* **22**, 569-574 (2007).
151. Rahbek, C. The role of spatial scale and the perception of large-scale species-richness patterns. *Ecology Letters* **8**, 224-239 (2004).
152. Hughes, A. C. et al. Sampling biases shape our view of the natural world. *Ecography* **44**, 1259-1269 (2021).
153. Raja, N. B. et al. Colonial history and global economics distort our understanding of deep-time biodiversity. *Nat. Ecol. Evol.* **6**, 145-154 (2022).
154. Hoorn, C., Perrigo, A. & Antonelli, A. *Mountains, Climate and Biodiversity* (John Wiley & Sons, 2018).
155. Chen, F. et al. The evolutions of the Yangtze River and its biodiversity. *The Innovation*, 100417 (2023).
156. Albert, J. S., Tagliacollo, V. A. & Dagosta, F. Diversification of neotropical freshwater fishes. *Annu. Rev. Ecol. Evol. Syst.* **51**, 27-53 (2020).
157. Waters, J. M., Craw, D., Youngson, J. H. & Wallis, G. P. Genes meet geology: fish phylogeographic pattern reflects ancient, rather than modern, drainage connections. *Evolution* **55**, 1844-1851 (2001).
158. Waters, J. M., Burridge, C. P. & Craw, D. River capture and freshwater biological evolution: A review of galaxiid fish vicariance. *Diversity* **12**, 216 (2020).
159. Albert, J. S. et al. Late Neogene megariver captures and the Great Amazonian biotic interchange. *Global Planet. Change* **205**, 103554 (2021).
160. Pfennig, K. & Pfennig, D. Character displacement: ecological and reproductive responses to a common evolutionary problem. *Q. Rev. Biol.* **84**, 253-276 (2009).
161. Waters, J. M. Competitive exclusion: phylogeography's 'elephant in the room'? *Mol. Ecol.* **20**, 4388-4394 (2011).
162. Rabosky, D. L. Diversity-dependence, ecological speciation, and the role of competition in macroevolution. *Annu. Rev. Ecol. Evol. Syst.* **44**, 481-502 (2013).
163. Abbott, R. et al. Hybridization and speciation. *J. Evol. Biol.* **26**, 229-246 (2013).
164. Taylor, S. A. & Larson, E. L. Insights from genomes into the evolutionary importance and prevalence of hybridization in nature. *Nat. Ecol. Evol.* **3**, 170-177 (2019).
165. Neuharth, D. et al. Evolution of rift systems and their fault networks in response to surface processes. *Tectonics* **41**, e2021TC007166 (2022).
166. Yuan, X. P., Braun, J., Guerit, L., Rouby, D. & Cordonnier, G. A new efficient method to solve the stream power law model taking into account sediment deposition. *J. Geophys. Res.: Earth Surf.* **124**, 1346-1365 (2019).
167. Acevedo-Trejos, E., Braun, J., Kravitz, K., Raharinirina, N. A. & Bovy, B. AdaScape 1.0: a coupled modelling tool to investigate the links between tectonics, climate, and biodiversity. *Geosci. Model Dev.* **16**, 6921-6941 (2023).
168. Yuan, X. P., Jiao, R., Dupont-Nivet, G. & Shen, X. Southeastern Tibetan Plateau growth revealed by inverse analysis of landscape evolution model. *Geophys. Res. Lett.* **49**, e2021GL097623 (2022).
169. Stokes, M. F. et al. Erosion of heterogeneous rock drives diversification of Appalachian fishes.

Science **380**, 855-859 (2023).
170. Cook, K. L., Andermann, C., Gimbert, F., Adhikari, B. R. & Hovius, N. Glacial lake outburst floods as drivers of fluvial erosion in the Himalaya. *Science* **362**, 53-57 (2018).
171. Nie, Y. et al. Glacial change and hydrological implications in the Himalaya and Karakoram. *Nat. Rev. Earth Environ.* **2**, 91-106 (2021).
172. Compagno, L., Huss, M., Zekollari, H., Miles, E. S. & Farinotti, D. Future growth and decline of high mountain Asia's ice-dammed lakes and associated risk. *Commun. Earth Environ.* **3**, 191 (2022).
173. Taylor, C., Robinson, T. R., Dunning, S., Rachel Carr, J. & Westoby, M. Glacial lake outburst floods threaten millions globally. *Nat. Commun.* **14**, 487 (2023).
174. Wang, W. et al. Abandonment of ancient cities near the Salawusu River valley, China, triggered by stream capture. *Commun. Earth Environ.* **3**, 326 (2022).
175. Bauer, P., Stevens, B. & Hazeleger, W. A digital twin of Earth for the green transition. *Nat. Clim. Change* **11**, 80-83 (2021).
176. Li, X. et al. Big Data in Earth system science and progress towards a digital twin. *Nat. Rev. Earth Environ.* **4**, 319-332 (2023).
177. Ramirez, R. M. & Craddock, R. A. The geological and climatological case for a warmer and wetter early Mars. *Nat. Geosci.* **11**, 230-237 (2018).
178. Galofre, A. G., Jellinek, A. M. & Osinski, G. R. Valley formation on early Mars by subglacial and fluvial erosion. *Nat. Geosci.* **13**, 663-668 (2020).
179. Stucky de Quay, G., Goudge, T. A., Kite, E. S., Fassett, C. I. & Guzewich, S. D. Limits on runoff episode duration for early Mars: Integrating lake hydrology and climate models. *Geophys. Res. Lett.* **48**, e2021GL093523 (2021).
180. Bamber, E. R., Goudge, T. A., Fassett, C. I., Osinski, G. R. & Stucky de Quay, G. Paleolake inlet valley formation: Factors controlling which craters breached on early Mars. *Geophys. Res. Lett.* **49**, e2022GL101097 (2022).
181. Mangold, N., Adeli, S., Conway, S., Ansan, V. & Langlais, B. A chronology of early Mars climatic evolution from impact crater degradation. *J. Geophys. Res.: Planets* **117**, E04003 (2012).
182. Goudge, T. A., Fassett, C. I., Head, J. W., Mustard, J. F. & Aureli, K. L. Insights into surface runoff on early Mars from paleolake basin morphology and stratigraphy. *Geology* **44**, 419-422 (2016).
183. Goudge, T. A., Fassett, C. I. & Mohrig, D. Incision of paleolake outlet canyons on Mars from overflow flooding. *Geology* **47**, 7-10 (2018).
184. Wordsworth, R. D. The Climate of Early Mars. *Annu. Rev. Earth Planet. Sci.* **44**, 381-408 (2016).
185. de Haas, T., Conway, S. J. & Krautblatter, M. Recent (Late Amazonian) enhanced backweathering rates on Mars: Paracratering evidence from gully alcoves. *J. Geophys. Res.: Planets* **120**, 2169-2189 (2015).
186. Farr, T. G. et al. The Shuttle Radar Topography Mission. *Rev. Geophys.* **45**, RG2004 (2007).
187. He, C. et al. A global dataset of the shape of drainage systems. *Earth Syst. Sci. Data Discuss.* https://doi.org/10.5194/essd-2023-363 (2023).
188. He, C. Tectonic control on the migration of the main drainage divide of a mountain belt: Constraints from numerical modeling and topographic analyses. *PhD thesis*, Zhejiang University (in Chinese with English abstract) (2021).
189. Karger, D. N. et al. Climatologies at high resolution for the Earth's land surface areas. *Sci. Data* **4**,

170122 (2017).
190. Jenkins, C. N., Pimm, S. L. & Joppa, L. N. Global patterns of terrestrial vertebrate diversity and conservation. *PNAS* **110**, E2602-E2610 (2013).
191. Lehner, B. & Grill, G. Global river hydrography and network routing: baseline data and new approaches to study the world's large river systems. *Hydrol. Processes* **27**, 2171-2186 (2013).

Acknowledgements

The authors thank Wolfgang Schwanghart, Maya F. Stokes, and Adam M. Forte for sharing the original data. The authors express their sincere gratitude to Jens Turowski, Eric Deal, Loraine Gourbet, Hannah Davies, and Amanda Wild for their insightful suggestions on the previous versions of this manuscript. The authors thank Yanyan Wang and Todd Ehlers for the insightful discussions. A special thanks to Lukas Becker for the improvement of English. C.H. acknowledges support from NSFC (National Natural Science Foundation of China) (Grant 42201008), Helmholtz-OCPC Postdoc Program (No. 202120), and the Expedition Funding from German Research Centre for Geosciences (Grant XP235501). J.B. and E.A-T. are supported by German Research Foundation (Grant 268236062) as part of the Collaborative Research Centre “Earth evolution at the dry limit” (CRC-1211). X.P.Y. acknowledges funding from NSFC (Grant 42272261).

Author contributions

C.H. wrote a first draft and drew figures. All authors contributed to the conceptualisation, discussion, data collection, and editing of all manuscript components.

Competing interests

The authors declare no competing interests.

Peer review information
Nature Reviews Earth & Environment thanks [Referee#1 name], [Referee#2 name] and the other, anonymous, reviewer(s) for their contribution to the peer review of this work.

Publisher's note
Springer Nature remains neutral with regard to jurisdictional claims in published maps and institutional affiliations.

Supplementary information
Supplementary information is available for this paper at https://doi.org/10.1038/s415XX-XXX-XXXX-X

Data availability

The locations of the natural examples on Earth and Mars (Google Earth files), as well as the raw data for Figs. 4d, 5b, 6, and Supplementary Figs. 2, 5, and 7, are available at: https://doi.org/10.6084/m9.figshare.21952820.v11.

Figures

Fig. 1 | **Drainage divides across scales**. **a** | Continental drainage divides (black) for North and South America, the European Alps, and the Southern Alps of New Zealand. Elevation data is from SRTM[186]. Drainage divides were sourced from Basin90m[187]. **b** | Catchment boundaries (yellow) in New Zealand, with river networks (blue). **c** | Secondary drainage divides acting as the boundaries of streams. Satellite imagery in panels b ©[2020] and c ©[2023] Google Earth. Drainage divides are among the most recognisable features on Earth’s surface, varying in spatial scale.

Fig. 2 | **The processes of gradual divide migration and river capture**. **a** | Dynamic divide movement

through gradual migration, which can be caused by differences in tectonics and erosion on either side of the divide. **b** | Bottom-up type river capture. Drainage divide is eroded by bottom-up headward erosion, connecting two river channels and resulting in river capture. **c** | Top-down type river capture. Divide is breached through top-down overflow erosion. Both types of capture can cause flooding downstream. **d** | An example of gradual divide migration where landslide and hillslope diffusion in Taiwan shifted a ridge. **e** | Divide migration through river capture at the northern margin of the Tibetan Plateau (triple vertical exaggeration). Refer to Supplementary Fig. 3a and the Data availability statement for the precise locations of the two examples. Satellite imagery in panels d and e ©[2022] Google Earth.

Fig. 3 | **Drivers of drainage divide motion.** Conceptual topographic profiles across drainage divides demonstrating the motion of divides under single drivers. Black arrows represent the direction of divide migration. These conceptual profiles apply at hillslope, catchment, and mountain range scales. **a** | Nonuniform tectonic uplift, denoted by the varying sizes of the red arrows, shifts the divide towards region with faster uplift. **b** | Horizontal advection can force the divide in the direction of advection, as marked by the red arrows. **c** | Where there are unequal slopes, the steeper side experiences more vigorous erosion, pushing the divide to the gently sloped side. **d** | Asymmetric erosion due to different rock types tends to push the divide to the side with a harder lithology. **e** | Erosional differences induced by unequal rainfall can push the divide to the side with less rain. **f** | The side with more glaciers erodes faster, moving the divide to the side with less glacial mass. In summary, divides tend to move to the side with slower erosion, faster uplift, or along the direction of horizontal advection.

Fig. 4 | **Stable position and migration rate of drainage divides. a** | Tectonic deformation and surface erosion affect the steady-state position of the main drainage divide of a convergent orogen. The motion of material underneath the Earth's surface, marked by dashed lines with arrows, can be separated into vertical uplift and horizontal advection. The landscape boundary condition (coastline) on the retro-wedge side is assumed to constantly align with the fixed plate boundary, which is the reference frame for divide motion. **b** | A conceptual relationship between convergence velocity and the stable position of the main divide, based on numerical simulations and analytical solutions[25,59,79]. The y axis is the steady-state fractional divide position, defined as the ratio of divide position (distance between the reference frame and the mountain center) and mountain width (the distance between the coastlines on both sides of the range). **c** | Steady-state fractional divide position as a function of the rainfall difference between two sides of the divide. Under horizontal advection, the mountain is asymmetric in steady state when there is no difference in rainfall ($x = 0$). **d** | Divide migration rates measured on Earth. Migration rates are from the Blue Ridge Mountains in the USA (n = 5)[3], east Australia (n = 1)[90], west India (n = 24)[81], east Madagascar (n = 15)[17], east Tibet (n = 29)[85], north Tibet (n = 43)[16], south Andes (n = 6)[36], and west Canada (n = 1)[88]. East Australia and west Canada only contain the range of divide migration rates, which are 0.04−0.08, and 4−10.7 mm yr^{-1}, respectively. Note that in Fig. 4d, the measurement of divide migration rate is with respect to the subsurface rock, which differs from that of Fig. 4a-c that are with respect to a fixed plate boundary. Divide migration rates typically range between 0.001 to 10 mm yr^{-1}, with an average of 0.6 mm yr^{-1}.

Fig. 5 | **Methods of judging divide migration direction.** Three methods for assessing drainage divide stability (left), each accompanied by a natural example (right). **a** | Divide migration by river capture can be identified from an elbow of capture with an upstream knickpoint. **b** | A capture elbow with upstream knickpoints illustrating a river capture event in China. Rivers 1−3 are Chaiwen River, Daotang River, and Yihe River[35]. Drainage network and river profile data are from SRTM[186]. **c** | χ-maps predict long-term divide mobility[32,115]. χ is a drainage-area normalised distance along a river. In the definition of χ equation, x is the distance from base level along the river; x_b is the x-coordinate of base level; A is the upstream drainage area; θ is reference channel concavity, with a global median of 0.43, ref.[109]. A reference drainage area (A_0) is introduced to give χ a unit of length[106]. **d** | χ-map predicts that the divide between the Roan Plateau and Colorado River is moving towards the plateau. **e** | Comparisons of cross-divide topographic relief can help predict short-term divide mobility. Histograms show the distribution of near-divide topographic reliefs. A strong contrast in relief between sides 1 and 2 predicts that the divide is migrating to side 1 with lower near-divide relief. A similar relief between sides 3 and 4 predicts a stable divide. **f** | Divide motion direction in the Big Bear Plateau predicted by the cross-divide relief agrees with the prediction from erosion rate[34]. The main drainage divide was cut into eight segments to calculate cross-divide relief separately. The erosion rate data are from ref.[34]. See Data availability statement or Supplementary Fig. 3a for the specific locations of the three natural examples. Panel a adapted from ref.[188]. Panel d adapted with permission from ref.[83], the Geological Society of America. All maps face

north except for the satellite image in panel d where a north arrow is present. Evidence of river capture can decode divide motion history, while topographic steepness metrics can predict future divide stability.

Fig. 6 | Effects of drainage divides on climate and biodiversity. a | The position of the main drainage divide affects rainfall, near-surface temperature, and the resulting species type and richness. Due to orographic precipitation effects, the windward side receives more rainfall and exhibits greater species diversity compared to the leeward side. **b** | The position of the main divide of the Himalaya affects rainfall and species richness, with increased rainfall and species richness on the windward side that is to the southern side of the divide. **c** | The position of the main divide of Madagascar influences rainfall and species richness, with increased rainfall and species richness on the windward side that is to the eastern side of the divide. Average annual rainfall data is from CHELSA[189]. Species richness here refers to the number of reported amphibians, mammals, and birds within a 100 km^2 area. Species richness data was integrated from BiodiversityMapping.org[190], with a resolution of 10 km. Elevation data is from SRTM[186]. The position of the main divide is from HydroSHEDS[191]. We used a 20-km wide swath in both the Himalaya and Madagascar to determine the average elevation, rainfall, and species richness along the profiles (see black box). Refer to Data availability statement for the specific locations of the profiles. **d** | A single river capture event can affect fish diversity, leading to dispersal, speciation, and extinction. The colour of fish is used to distinguish different species. A landscape-biodiversity coupled simulation on the right shows the evolution of fish richness in the expanding and shrinking basins in response to a single capture event[97]. River captures can enhance species richness in the expanding basins but reduce biodiversity in the shrinking catchments.

Glossary

Base level
The regional lowest point above which a river can erode its channel, such as the ocean or a lake.

Biodiversity
The variety of lifeforms, including their genetic, phenotypic, functional, taxonomic, and ecological variation in space and time.

Catchments
Geographical areas where surface water flows and converges into common drainage points.

Digital twin
A digital model that uses real-time data and simulation to replicate the behaviour of a physical system or process, enabling optimisation and predictive maintenance.

Expanding catchment
Catchment that gains drainage area from their neighbours during divide migration.

Hillslopes
The sloping surfaces of hills located between river channels and drainage divides.

Impact crater rim
A raised boundary encircling an impact crater, often functioning as drainage divide.

Knickpoint
A sharp change in the slope of river profile, such as a waterfall.

Main drainage divide
Drainage divide that separates multiple drainage basins.

Rift margin escarpments
Cliffs formed along the edge of rift valleys where the Earth's crust pulls apart.

Shrinking catchment
Catchment that loses drainage area during divide migration.

Thermochronology
A geological dating technique that determines the temperature history of rocks, revealing the timing of tectonic and erosional events.

Horizontal tectonic advection
The movement of topography in a horizontal direction induced by tectonic deformation.

Wind gap
A drainage divide through which a waterway once flowed is now dry due to river capture.

Fig 1

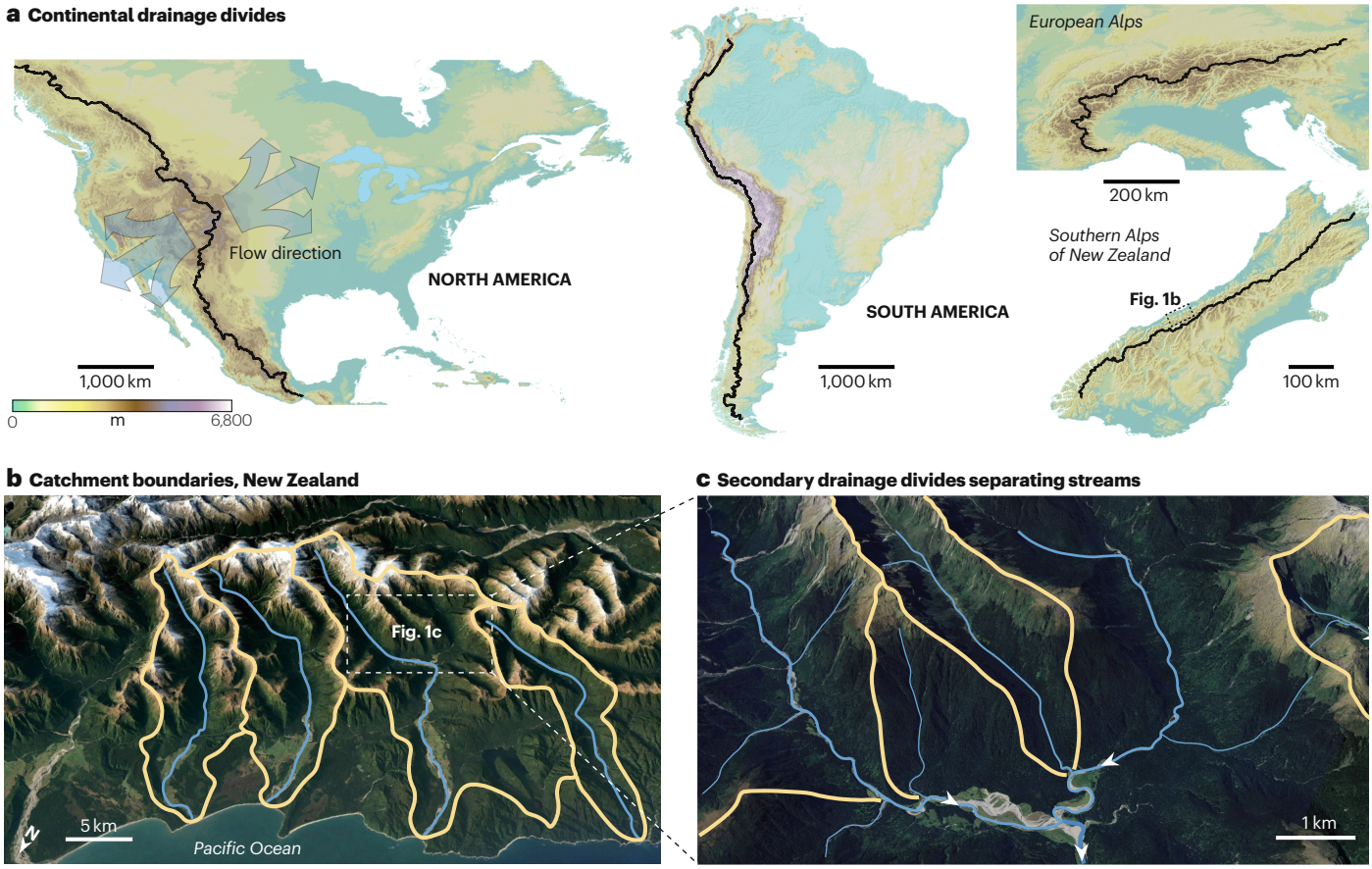
a Continental drainage divides
Flow direction
NORTH AMERICA
1,000 km
0
m
6,800
SOUTH AMERICA
1,000 km
European Alps
200 km
Southern Alps
of New Zealand
Fig. 1b
100 km
b Catchment boundaries, New Zealand
Fig. 1c
5 km
Pacific Ocean
c Secondary drainage divides separating streams
1 km

Fig 2

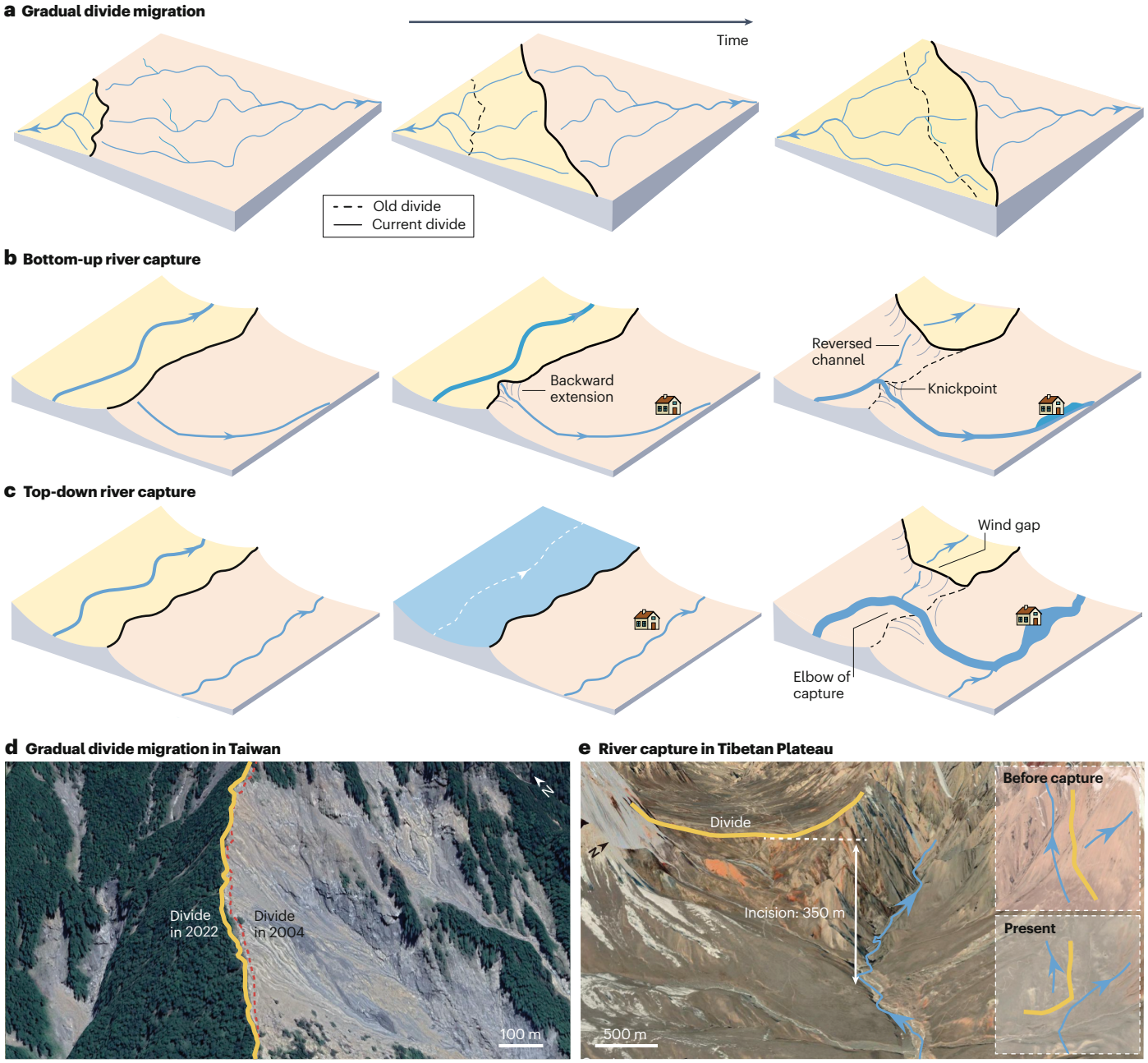
a Gradual divide migration
Time
Old divide
Current divide
b Bottom-up river capture
Backward extension
Reversed channel
Knickpoint
c Top-down river capture
Wind gap
Elbow of capture
d Gradual divide migration in Taiwan
Divide in 2022
Divide in 2004
N
100 m
e River capture in Tibetan Plateau
Divide
Incision: 350 m
N
500 m
Before capture
Present

Fig 3

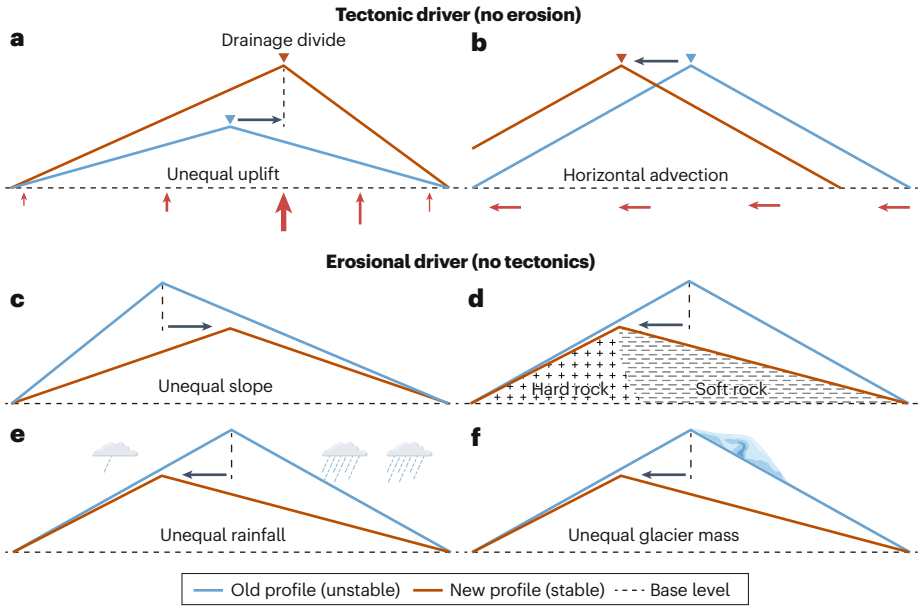
Tectonic driver (no erosion)
a
Drainage divide
Unequal uplift
b
Horizontal advection
Erosional driver (no tectonics)
c
Unequal slope
d
Hard rock
Soft rock
e
Unequal rainfall
f
Unequal glacier mass
Old profile (unstable)
New profile (stable)
Base level

Fig 4

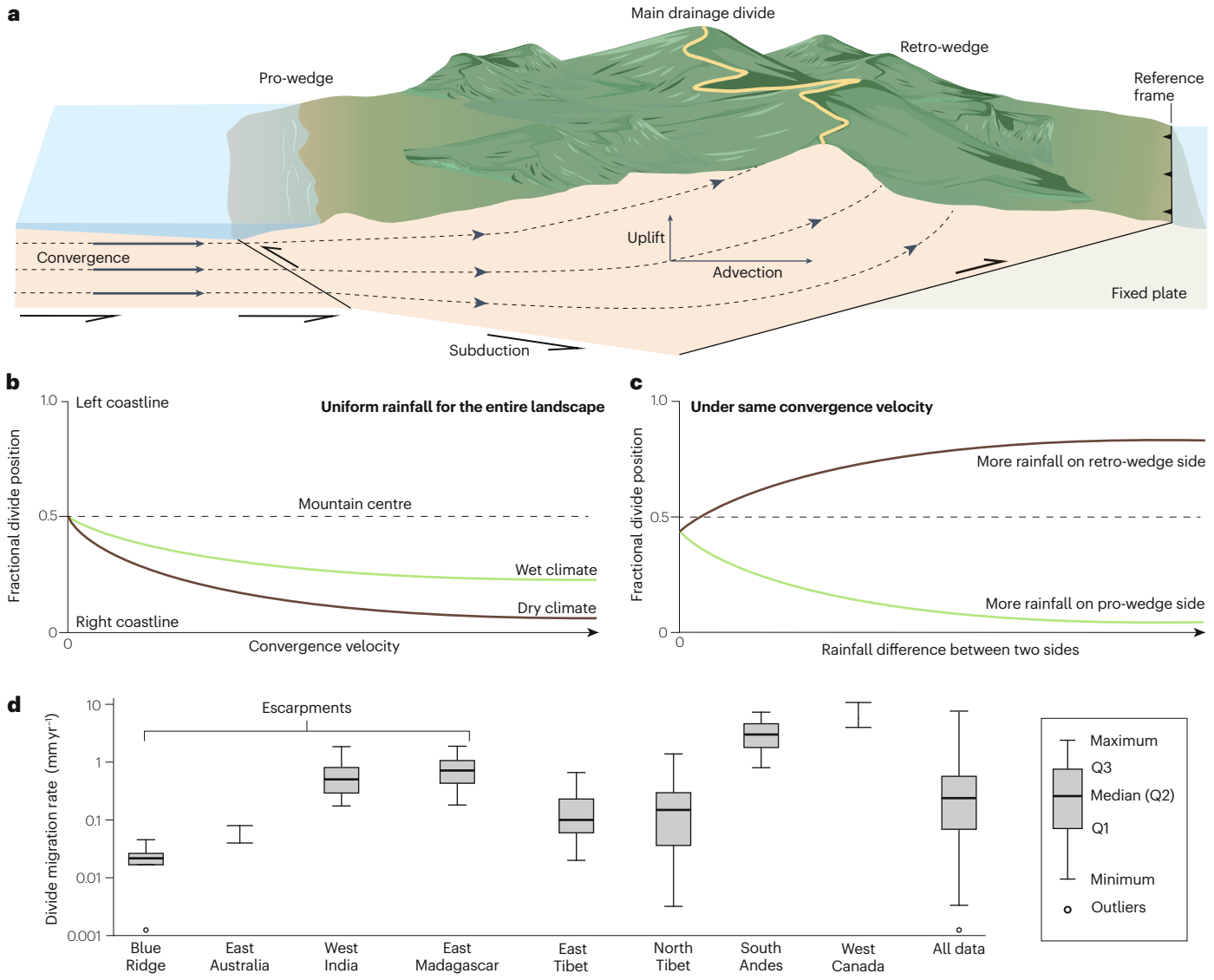
a
Main drainage divide
Retro-wedge
Pro-wedge
Reference frame
Convergence
Uplift
Advection
Fixed plate
Subduction
b
Left coastline
Uniform rainfall for the entire landscape
Fractional divide position
1.0
0.5
0
Mountain centre
Wet climate
Dry climate
Right coastline
0
Convergence velocity
c
Under same convergence velocity
Fractional divide position
1.0
0.5
0
More rainfall on retro-wedge side
More rainfall on pro-wedge side
0
Rainfall difference between two sides
d
Escarpments
Divide migration rate (mm yr⁻¹)
10
1
0.1
0.01
0.001
Blue Ridge
East Australia
West India
East Madagascar
East Tibet
North Tibet
South Andes
West Canada
All data
Maximum
Q3
Median (Q2)
Q1
Minimum
Outliers

Fig 5

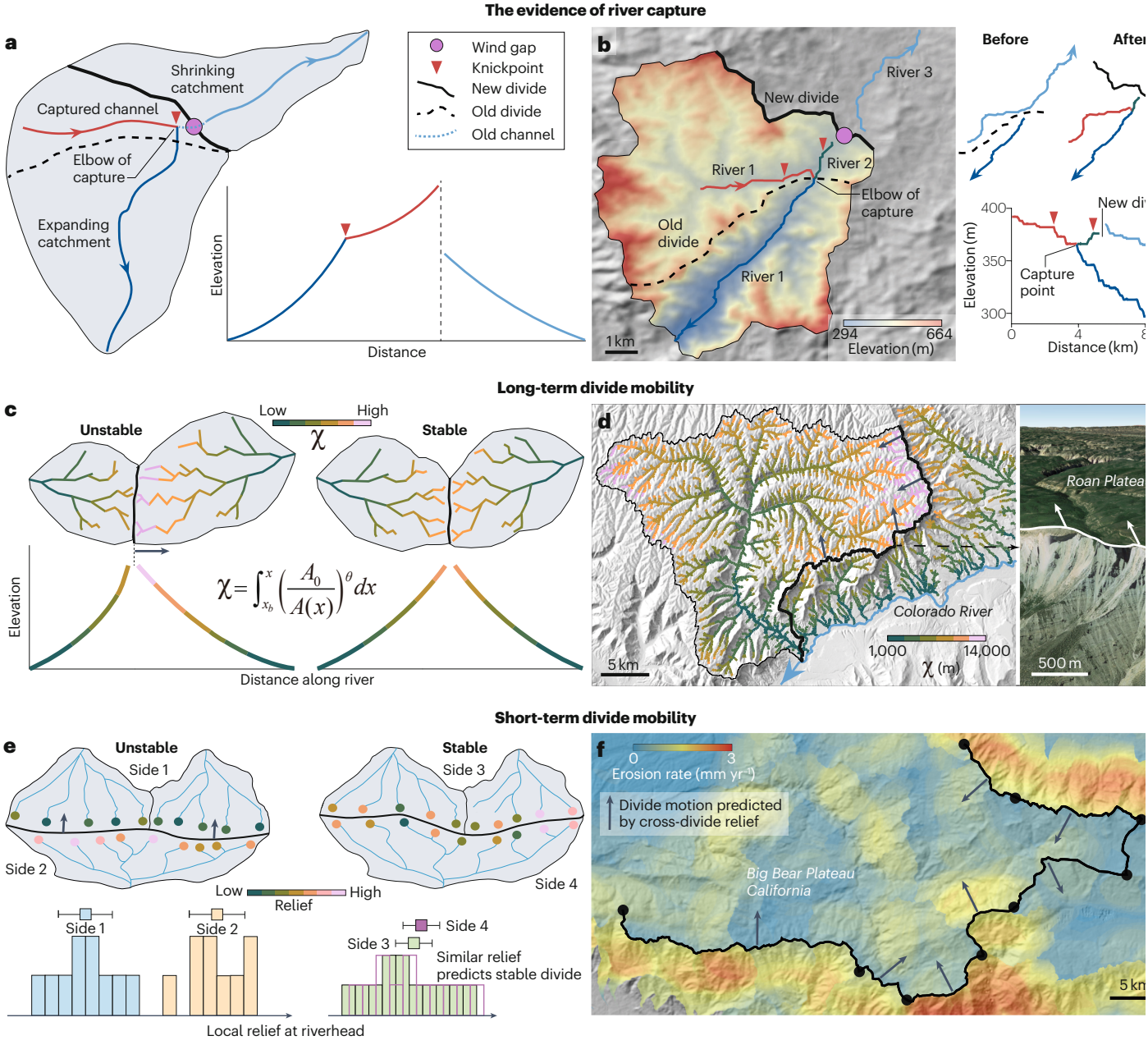
The evidence of river capture
a
Shrinking catchment
Captured channel
Elbow of capture
Expanding catchment
Wind gap
Knickpoint
New divide
Old divide
Old channel
Elevation
Distance
b
New divide
River 3
River 1
River 2
Elbow of capture
Old divide
River 1
1 km
294
664
Elevation (m)
Before
Aft
400
350
300
Elevation (m)
New di
Capture point
0
4
Distance (km)
Long-term divide mobility
c
Unstable
Low
High
χ
Stable
Elevation
$\chi = \int_{x_b}^{x} \left(\frac{A_0}{A(x)}\right)^{\theta} dx$
Distance along river
d
Roan Platea
Colorado River
5 km
1,000
14,000
χ (m)
500 m
Short-term divide mobility
e
Unstable
Side 1
Side 2
Stable
Side 3
Side 4
Low
High
Relief
Side 1
Side 2
Side 4
Side 3
Similar relief predicts stable divide
Local relief at riverhead
f
0
3
Erosion rate (mm yr⁻¹)
Divide motion predicted by cross-divide relief
Big Bear Plateau
California
5 km

Fig 6

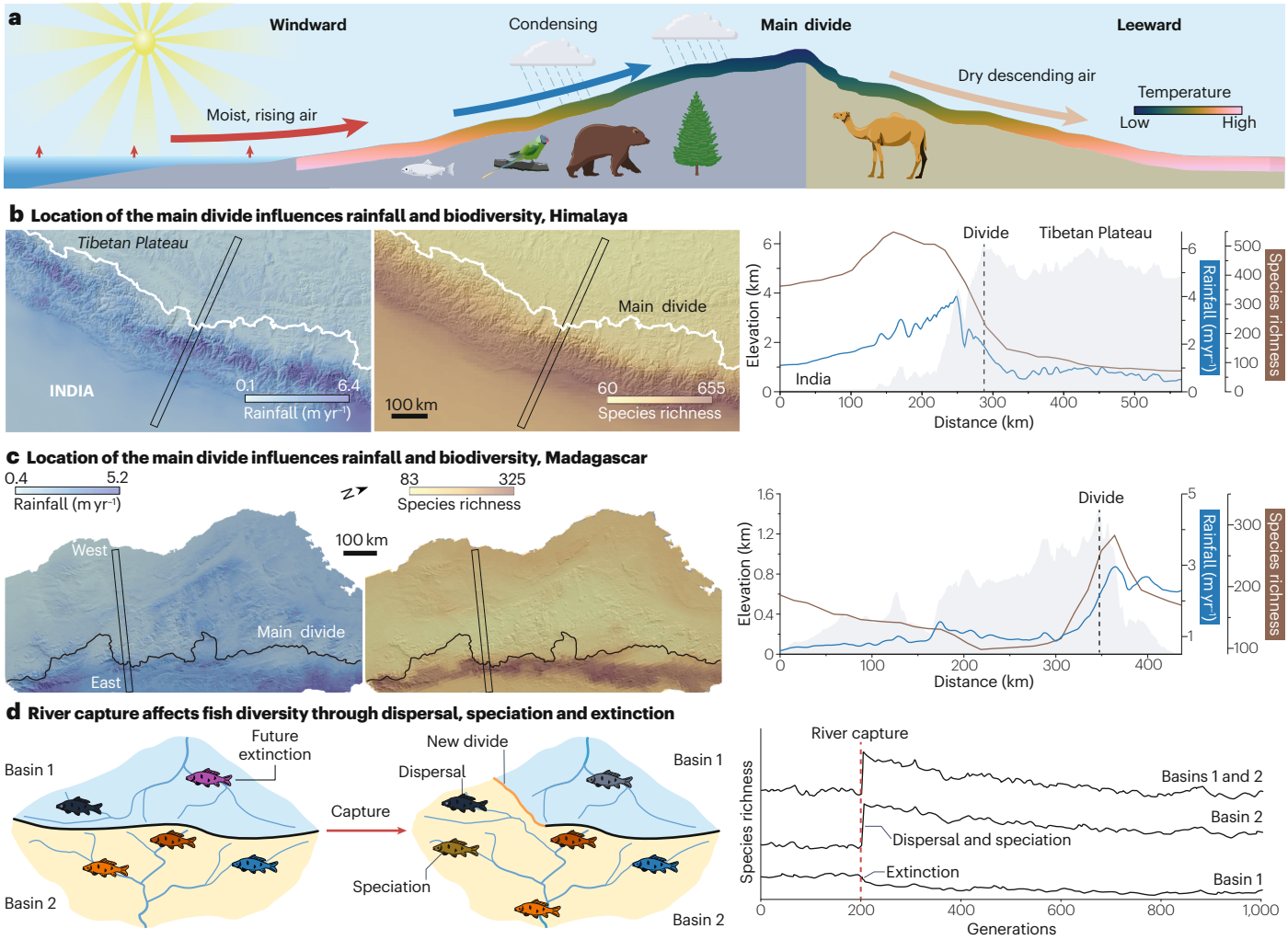
a
Windward
Condensing
Main divide
Leeward
Moist, rising air
Dry descending air
Temperature
Low
High
b Location of the main divide influences rainfall and biodiversity, Himalaya
Tibetan Plateau
INDIA
0.1
6.4
Rainfall (m yr⁻¹)
100 km
Main divide
60
655
Species richness
Divide
Tibetan Plateau
Elevation (km)
India
Rainfall (m yr⁻¹)
Species richness
Distance (km)
c Location of the main divide influences rainfall and biodiversity, Madagascar
0.4
5.2
Rainfall (m yr⁻¹)
83
325
Species richness
100 km
West
Main divide
East
Divide
Elevation (km)
Rainfall (m yr⁻¹)
Species richness
Distance (km)
d River capture affects fish diversity through dispersal, speciation and extinction
Basin 1
Future extinction
Basin 2
Capture
New divide
Dispersal
Speciation
Basin 1
Basin 2
River capture
Species richness
Basins 1 and 2
Basin 2
Dispersal and speciation
Extinction
Basin 1
Generations